

Lasers and Optical Diagnostics for Next Generation IC Engine Development: Ushering New Era of Engine Development

Avinash Kumar Agarwal and Akhilendra Pratap Singh

Abstract Researchers are trying to improve engine efficiencies and emission characteristics in an extremely challenging environment. This demands complying with ever-increasingly tightening emission norms and fuel economy norms globally, which are the prime forces driving the automotive industry globally. Optical diagnostic techniques have emerged as a valuable tool in development of engine powertrain and emission control technologies in last one decade. This chapter deals with variety of optical diagnostic techniques such as particle image velocimetry (PIV), phase Doppler interferometry (PDI) and endoscopy, applied to internal combustion (IC) engines. Laser based measurements in real time in the engine combustion chamber have ushered a new era of research for finding answers to some of the most intriguing in-cylinder processes, which were only speculated until recently. These optical diagnostic techniques have enabled engine researchers to sharpen their modeling tools using experimental data from realistic geometry engines firing under varying loads. Fuel-air mixing and combustion are mainly affected by in-cylinder air-flow and fuel spray characteristics. Air-flow structures developed inside the engine combustion chamber significantly influence the fuel-air mixing process. For validate this phenomenon, researchers investigated in-cylinder air-flow characteristics of motored engine using time-resolved tomographic particle imaging velocimetry (TPIV). Fuel spray characteristics could be determined using PDI, which provides information about droplet size distribution and 3D-velocity distributions. To gain visual access to the combustion process in a production engine's combustion chamber at high loads, another optical diagnostic technique "engine endoscopy" can be used, which can enable spatial combustion visualization, soot distribution as well as temperature distribution.

Keywords In-cylinder flow-field • Fuel sprays • Phase doppler interferometry • Engine endoscopy • Flame-temperature distribution • Soot distribution

A.K. Agarwal (✉) · A.P. Singh
Indian Institute of Technology Kanpur, Kanpur, India

© Springer Nature Singapore Pte Ltd. 2017
A.K. Agarwal et al. (eds.), *Combustion for Power Generation and Transportation*, DOI 10.1007/978-981-10-3785-6_11

211

1 Introduction to Optical Diagnostics

Internal combustion (IC) engines are an important technology, affecting human life for more than a century. Reliability and efficiency improvement in IC engine were the two domains of improvement until the 20th century however in the 21st century the focus has shifted to exhaust gas emissions control and fuel consumption reduction. Increasing concerns about the environmental degradation and human health due to the harmful gases emitted from IC engines have imposed relatively stricter emission regulations for automotive manufactures. In 1970, Clean Air Act (1970) of the EPA started the new paradigm for control of emission levels, which became more stringent in successive norms. Numerous techniques such as turbocharging, exhaust gas recirculation (EGR), high speed direct injection (HSDI), gasoline direct injection (GDI), low temperature combustion (LTC) and after-treatment devices have been developed and implemented in IC engines in order to optimize the combustion and reduce emission. However, these techniques have their own limitations. Many researchers focused on in-cylinder conditions to improve combustion by controlling the fuel injection parameters and in-cylinder flows. They looked at injection parameters such as fuel injection pressure (FIP) and start of injection (SoI) timings along with injector nozzle configuration, which directly influence the spray characteristics such as spray tip penetration, spray cone angle, droplet size distribution, etc. These spray characteristics play an important role in fuel-air mixing and affect engine combustion, performance and emissions characteristics.

Therefore detailed investigation of in-cylinder characteristics becomes important for further improvement of IC engine performance and emissions reduction. Over the years, different optical diagnostics techniques have been developed to visualize and understand the in-cylinder phenomenon of IC engines in which laser based techniques such as particle image velocimetry (PIV) and phase Doppler interferometry (PDI) are the most important ones. These methods are well-known for their high temporal and spatial resolution. In most of these methods, the measurements are based on light and molecule interactions. This interaction generates a signal, which depends on the molecule's state and their quantity. Generated signal is acquired and processed to obtain specific in-cylinder information. Main difficulty with these methods in IC engines is to gain optical access. In the early years of research, probes were used to gain insights into the combustion chamber. However probes themselves may affect/ alter the actual physical condition in the measurement volume, leading to unreliable results. Use of existing ports, small optical windows, endoscopes and transparent cylinder liners has made these optical techniques possible for IC engine diagnostics. In IC engines, in-cylinder processes are mainly controlled by fluid flows such as air-flow, fuel-air mixing, flow of combustion products, etc. Recent upgrades in computing power have established Computational Fluid Dynamics (CFD) as a key design tool in fluid mechanics. Most CFD models are close approximation to a given fluid flow, but they generally require experimental validation because these flows cannot be simulated without

appropriate boundary conditions. Combustion in IC engines is far from fully understood and there are complete lack of understanding about formation of pollutants and oxidation within the engine combustion chamber, which needs to be better understood. Considering the pollutant formation inside the combustion chamber, the fuel-air mixing is of paramount importance for emission reduction. Optimized fuel-air mixing is fundamentally dependent on the charge air motion inside the engine cylinder. Therefore the focus is set on understanding the connections between spray process and the formation of pollutants such as soot particles and unburned hydrocarbons using optical diagnostics. It also becomes important to study and understand the air-flow behavior inside the combustion chamber of a modern diesel engine. Engines modified for optical studies, allowing optical access to the combustion chamber have been used in different investigations, and these have been presented in this chapter. This chapter is focused on understanding different in-cylinder processes such as spray diagnostics, air-flow characteristics, fuel-air mixing, combustion and emission formation.

2 Air-Flow Characterization

In-cylinder air-flow of an engine is mainly governed by the intake manifold, valve design and piston geometry. Air induced in the intake stroke of an engine cycle interacts with the piston and cylinder walls to form complex 3-D flow structures. These flow structures affect the fuel-air mixing, fuel distribution and heat transfer from the engine cylinder, which directly influences the engine performance. These in-cylinder flow structures can be controlled by several parameters such as inlet manifold design, cylinder head and piston crown geometry. Different geometries such as helical intake port, directed intake port, flat-crown piston and concave crown piston have been explored to improve the air flow. Engine speed and piston position also strongly affect in-cylinder flow characteristics and it is reported that large flow structures formed in the intake stroke distort and breaks into smaller structures in later stages of the compression stroke, which enhances turbulence at the time of fuel injection [27]. Figure 1 shows that average velocity of inlet air is significantly higher at higher engine speeds, however during the compression stroke, the difference between average air velocities at different engine speeds reduced.

Swirl and tumble are commonly known flow structures generated inside the cylinder. These flow structures are vortices with axis of rotation being parallel and perpendicular to the cylinder axis respectively. Swirl is believed to survive the compression stroke with increasing angular velocity, while tumble is known to break into smaller flow structures of high turbulence intensity near TDC [34]. Combination of these flow patterns produces complex and highly turbulent flow structures. These flow structures lead to more uniform fuel distribution, resulting in leaner engine operation. However, this can lead to misfire in case of SI engine because bulk motion causes charge to redistribute away from the spark plug. For CI

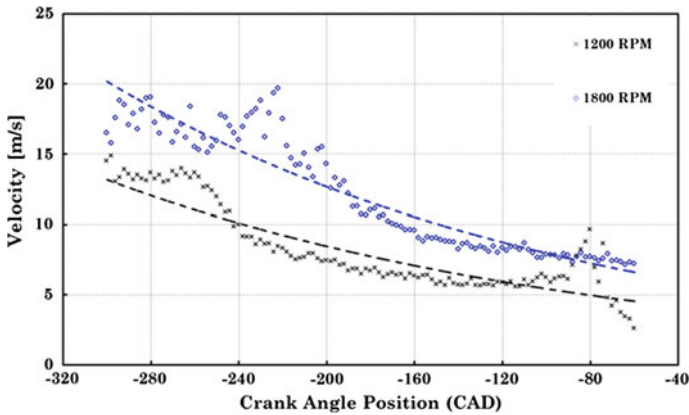


Fig. 1 Average velocity variation at 1200 and 1800 rpm during intake and compression stroke [27]

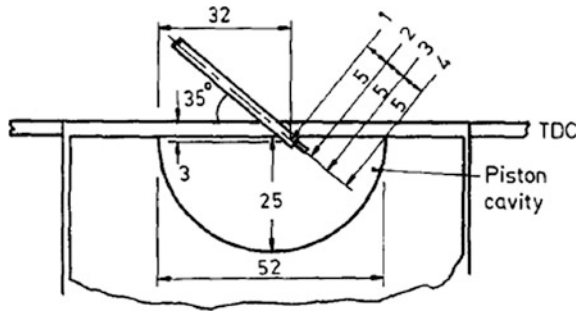
engines, turbulence is beneficial to a certain extent because current engine technology requires different level of turbulence according to their operating conditions. Implementation of different engine modifications and techniques to enhance the air motion result in decreased volumetric efficiency. Therefore it becomes important to quantify the in-cylinder flows.

2.1 Air-Flow Characterization Techniques

Different methods have been used by researchers to measure and visualize the in-cylinder air-flow characteristics. Hot wire anemometry (HWA), laser Doppler anemometry (LDA) and PIV are widely known methods for flow measurements. HWA is an old method used for studying laminar, transitional and turbulent flows. This is an intrusive velocity measurement technique, which provides flow information at a single point in the flow-field. Subramanian et al. [86] used HWA in a high compression diesel engine to obtain quantitative flow information. They analyzed the effects of engine speed and compression ratio on mean velocity and turbulence intensity. They used DISA 55M10 CTA bridge in combination with a DISA 55A75 high temperature hot-wire probe for velocity measurement at four positions inside the piston cavity. Figure 2 shows the positions of probes inside the engine combustion chamber.

LDV is another non-intrusive velocity measurement technique, which gives velocity information at a single point of interest. In this technique, two coherent laser beams are made to intersect at the point of measurement to form a fringe pattern. The tracer particles in the seeded flow pass through the fringe pattern and scatter light. The scattered light is received by a photomultiplier. The frequency of the scattered light depends on the particle velocity. By comparing changes in the frequency of the incident and the scattered light, the particle velocity is calculated.

Fig. 2 HWA probe positions for in-cylinder velocity measurement [88]



Chan [14] applied LDV for 2-component and 3-component velocity measurements in a motored SI engine. For 3-component velocity measurement, all six laser beams were guided into the cylinder volume through a semi-circular window incorporated in the cylinder head. The axial, radial and tangential velocity components were measured at different crank angle positions (Fig. 3).

They also described the difficulties in applying LDV in IC engines. In spite of advantages such as non-intrusive to the flow, directional sensitivity and high temporal resolution, LDV technique deals with only a small area in the flow-field. Thus volumetric flow visualization of large area becomes difficult for LDV technique, which is a severe limitation. PIV is a non-intrusive volumetric flow visualization method, which resolved difficulties experienced in conventional

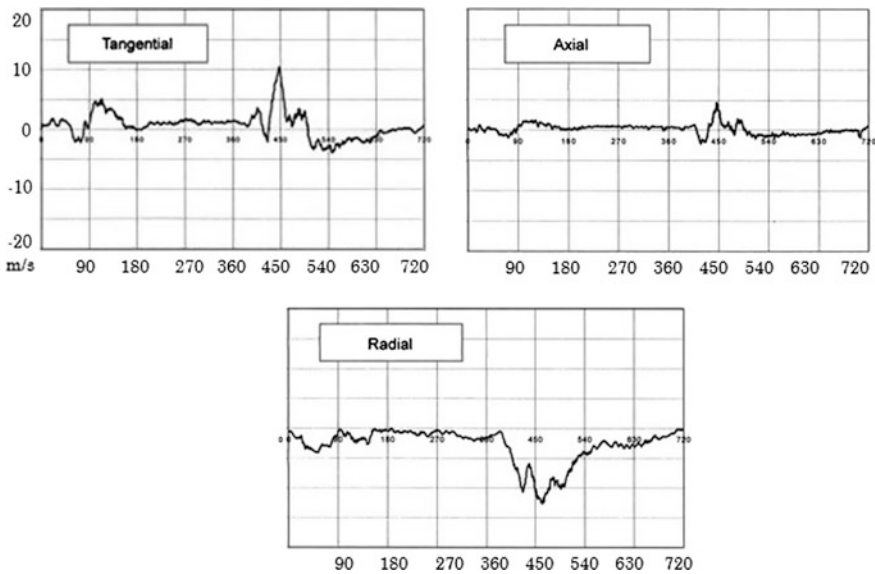


Fig. 3 Three component velocity data (Tangential, axial and radial) using LDV [14]

techniques and emerged as an effective flow measurement technique. Tomographic particle imaging velocimetry (TPIV) can be used to investigate the in-cylinder flow characteristics within a volume.

2.2 Particle Imaging Velocimetry (PIV)

PIV is an optical, indirect flow visualization and measurement technique, in which illuminated tracer particles are captured on a photographic film or digital camera and captured images are further processed to obtain instantaneous velocity field. In this visualization technique, flow-field is seeded with small tracer particles, which are believed to faithfully follow the flow. The area of interest in the flow-field is illuminated by a double pulsed, high intensity laser sheet at two instant with small time lag between them. Light scattered by the tracer particles is captured by cameras, usually placed at 90° to the illumination plane. Triggering of these cameras is synchronized with laser pulses using an external synchronizer. For the flow-field acquisition, cameras can be operated either in single frame mode (Flow-field for consecutive illuminations is captured on a single frame) or double frame mode (separate frames are used for each illumination). Acquired recordings are post-processed by dividing each image into small interrogation regions, which are auto-correlated or cross-correlated to obtain average displacement vectors of tracer particles in photographic coordinates. These camera scale displacements are converted into global coordinates by using a calibration process. Further, with known time separation between consecutive laser illuminations, velocity vectors in the area of interest are calculated. Depending on the experimental requirements and desired data from the flow-field, the nature and fundamental requirements of PIV setup changes. These requirements include seeder material, laser pulse energy, pulse separation, laser thickness and camera settings. A general schematic of PIV setup is shown in Fig. 4.

2.3 PIV Configurations

Different arrangements, such as 2-D PIV, time-resolved PIV, stereo PIV, holographic PIV and TPIV are developed with the passage of time for 2-component and 3-component velocity measurements either in a plane or volume. It is possible to perform TPIV measurements using 2 camera projections [55]. Various researchers implemented PIV for flow analysis in diverse experiments [7, 8, 81, 83, 96, 98]. Wernert et al. [95] applied the PIV for flow-field analysis around an aero foil. Kawaguchi et al. [45] studied the spatial velocity distribution of drag reducing surfactant in a 2-D channel the PIV technique. Reeves et al. [69] applied PIV in a four-valve, optical engine to study large-scale flow structures. Depending on the experimental setup, there are numerous variations in PIV arrangement.

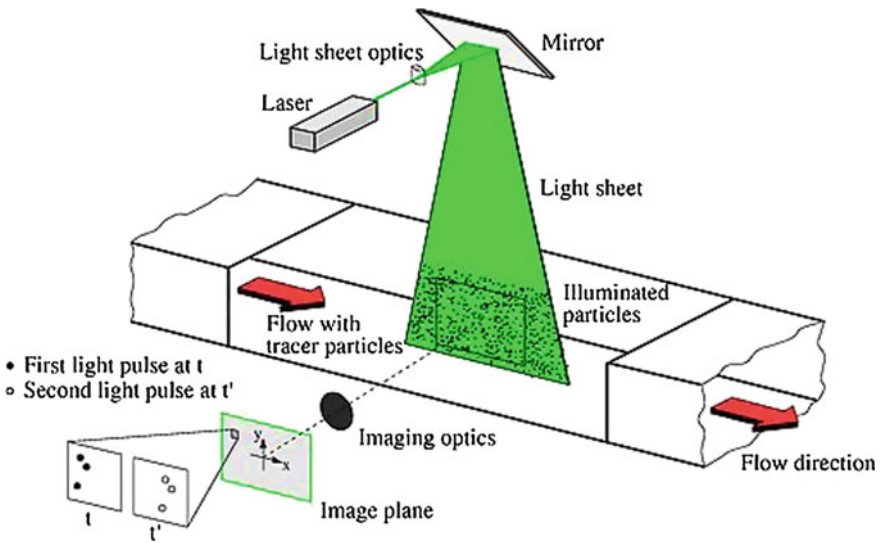


Fig. 4 Typical PIV setup for flow velocity measurements [37]

2-D PIV (2D-2C) is the most common PIV arrangement used for planar flow measurements and visualization. In this technique, the illuminated 2-D flow-field is captured on two consecutive images. These images are further auto-correlated or cross-correlated to obtain the flow velocity information. This technique gives 2-components of the planar velocity vectors. Time-resolved PIV is similar to 2-D PIV, except that instead of a single pair of images, it takes a number of image pairs, thus providing temporal development of the flow-field. The limitation of this technique is the acquisition speed of the camera, i.e. the time delay between the successive image pair capture. With rapid development in camera technology, the temporal resolution of PIV technique is expected to increase. Stereoscopic PIV (2D-3C) removes the inability of 2-D PIV to measure the 3rd, out-of-plane component of the flow velocity. It uses 2 cameras with different viewing directions to capture the illuminated flow-field. The three-components of velocity vectors are calculated by using images from both cameras. For calculation of 3rd velocity component, both these cameras are required to focus on the same plane in the acquisition flow-field.

Holographic PIV (3D-3C) allows 3-D measurement of all three velocity components. In this technique, the positions of tracer particles are recorded on the holographic plate by making the scattered light of seeders to interfere with the reference laser beam. This generates a hologram, which can be used to reconstruct the flow-field by illuminating it with the original reference beam. This reconstructed flow-field is interrogated using 3-D cross-correlation to obtain velocity field. Despite advantages 3D-3C velocity measurement, issues such as distortions in reconstructing the flow-field, speckle noise, coherent imaging degrades the

holographic PIV results. TPIV is another 3D-3C velocity measurement technique. Velocity measurement principle used in TPIV is same as 2D PIV, except the fact that the flow-field projections are captured by several cameras. These projections are further used to reconstruct the 3-D flow-field. This 3-D flow-field is analyzed by 3-D cross-correlation, in order to calculate the 3-D three component velocity field. Foundation of TPIV is based on algorithm used to reconstruct the 3-D field. Generally TPIV uses the “Multiplicative Algebraic Reconstruction Technique” (MART) to reconstruct three dimensional flow-field. TPIV technique with 2 cameras has been implemented in this study for in-cylinder flow analysis in a CI engine.

2.4 Application of PIV

In the early years of PIV development for IC engines, it was difficult to gain the in-cylinder access while keeping the modified engine geometry and working close to the actual engine. Different techniques such as endoscopy, small optical windows, engine head ports and valves were used to visualize the engine flows. Sweetland and Reitz [89] applied the planar PIV technique to measure gas velocity and turbulence inside the piston bowl of a motored diesel engine. In this study, in-cylinder optical access was gained through the fuel injector port and the exhaust valve. The seeder particles of TiO_2 were illuminated using a Nd:YAG laser, which was guided through the injector port. The flow images were captured on photographic film for flow visualization. To validate PIV measurements, the acquired turbulent jet data were compared with the measurements made using conventional techniques and the simulation results using KIVA-3 code. Though the measurement was affected by the out-of-plane velocity component, it was inferred that the high and low estimates of turbulence intensity can be obtained from these limited PIV measurements. Flows inside a specific geometry can also be visualized by using the endoscopic technique. Nishiyama et al. [61] applied endoscopic stereo PIV to study the exhaust gas flow in the exhaust manifold of an SI engine. It is believed that the impingement of exhaust flow on the oxygen sensor and the catalyst affected the engine performance. A special twin-endoscope and optical window arrangement was developed to investigate the exhaust gas flow. The developed endoscopic stereo PIV system was tested on a steady flow rig and the results were compared with HWA, LDV and 2-D PIV measurements.

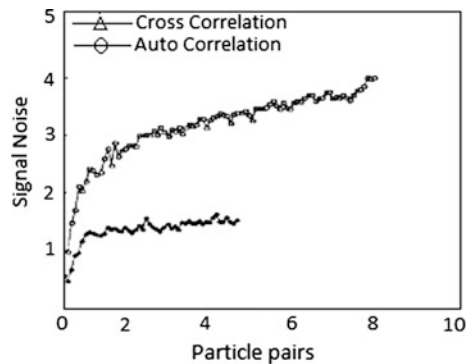
In the early days of development of PIV, photographic films were used for image acquisition and auto-correlation was used for image evaluation, which resulted in directional ambiguity. Reeves et al. [69] applied auto-correlation based 2-D PIV for in-cylinder flow measurements and visualization in a SI engine. They derived the velocity vector maps in vertical and horizontal planes for different crank angle positions. Their study discussed the difficulties experienced in implementing PIV in the engines. The flow images of olive oil droplets, illuminated by Nd:YAG laser were acquired on a photographic film. In-cylinder flow visualization revealed breakdown of large-scale flow patterns into homogeneous micro-turbulence, due to

distortion and shear as the cycle progressed from the intake to the compression stroke. To remove the directional ambiguity of the velocity data, different techniques were used. Stucky et al. [85] used two-color planar PIV to remove this kind of ambiguity in the velocity data from the engines. This study analyzed implementation of planar PIV in IC engines and reported the advantages of cross-correlation over auto-correlation technique using computer simulations. They also investigated the importance of cross-correlation over auto-correlation by analyzing the effects of seed density on signal-to-noise ratio of auto and cross-correlation techniques. They found significantly higher signal-to-noise ratio for cross-correlation compared to auto-correlation (Fig. 5).

Developments in digital photography and computational power changed the method of image acquisition from conventional photographic film to digital cameras. Reeves et al. [69] showed the application of 2-D digital PIV in an engine, which allowed acquisition of thousands of flow visualization sequences and velocities at different crank angle positions. Their results showed that swirl center drifted and flow patterns changed significantly with crank angle. The observed flow structures were further studied to understand the cyclic variability. Though the recorded digital PIV data was of reduced accuracy and lower spatial resolution, it provided the quantification of major flow structures inside the engine cylinder.

Significant effects of in-cylinder flows on engine performance and emissions have led researchers to improve the engine flow patterns by changing the engine design. The in-cylinder flow-field is mostly affected by the intake manifold geometry, valve and piston shapes. Some of the flow-field affecting designs are helical inlet, directed inlet, shrouded valve, masked valve, deep and shallow bowl piston, flat crown and concave piston. Intake valves being the only energy source for in-cylinder flows, analysis of flows near the intake valve during its opening and closing is of considerable importance. Lee and Farrell [52] investigated the two dimensional flow-field near the intake valves using 2-D PIV, and studied the unsteady effects of the cam-speed and valve lift on flows near intake valve. The flow measurements were obtained at valve half open (during opening), fully open intake valve, valve half open (during closing) and after full valve closure. Their

Fig. 5 Effect of seed density on signal-to-noise ratio [87]



results showed that the intake jet velocity increased with increasing cam angle. The comparison of dynamic and static valve flow at same valve lift and pressure drop across the intake valve showed that the static valve flow has higher velocity than the dynamic valve. The flow study also showed the cyclic variations in flow patterns and these variations were reduced with high intake jet velocity. Valentoni et al. [91] extended this research to obtain better 3-D flow patterns around the valve. They analyzed the flow in a certain valve area. Flow patterns from these measurement planes showed the development of wall jet type of flow on the backside of the valve. This study also showed that in case of two intake valves, flow from one of the intake valves dominated the initial flow. Figure 6 shows the velocity map of fully open inlet valve at 500 rpm.

Huang et al. [40] analyzed the inception, establishment, development and destruction of in-cylinder flow structures of a two-valve, motored engine with a flow deflection valve in the intake manifold. The flow structures were quantified by swirl and tumble ratio using PIV measurement. The flow data were correlated with the engine performance to show the effect flow has on the engine combustion. The deflection valve was found to generate high tumble and swirl structures inside the cylinder, while without inlet stream deflection, no swirl and tumble effects were observed. The valve deflection was also noticed to produce positive effects on the engine power and torque. Similar research was performed by Perini et al. [67] using a CFD model. The effects of variable throttle orientation in the intake manifold to generate swirl motion were obtained using KIVA code and the same were validated using PIV measurements. Justham et al. [44] studied the inter-relationship of intake manifold design and in-cylinder flow-fields by implementing digital PIV setup on a motored SI engine. They reported that the relationship between flow-field intake runner and cylinder was stronger during the intake stroke however it died out in compression stroke due to breakdown of large-scale motions. Large-scale bulk motions were affected by cyclic variations in the intake flow. Figure 7 shows that

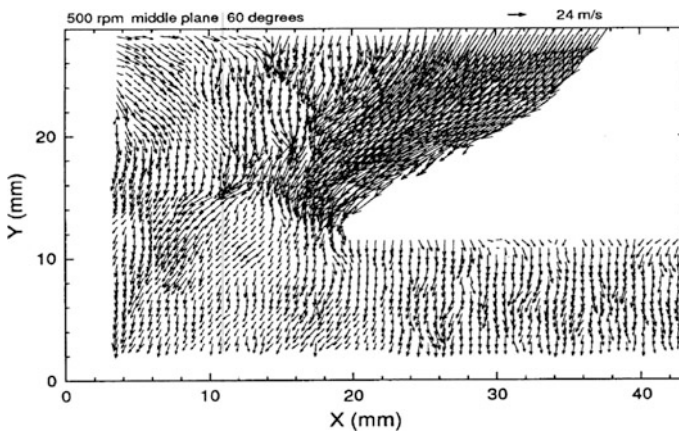


Fig. 6 Velocity map in the center plane of inlet valve at 60° aTDC [52]

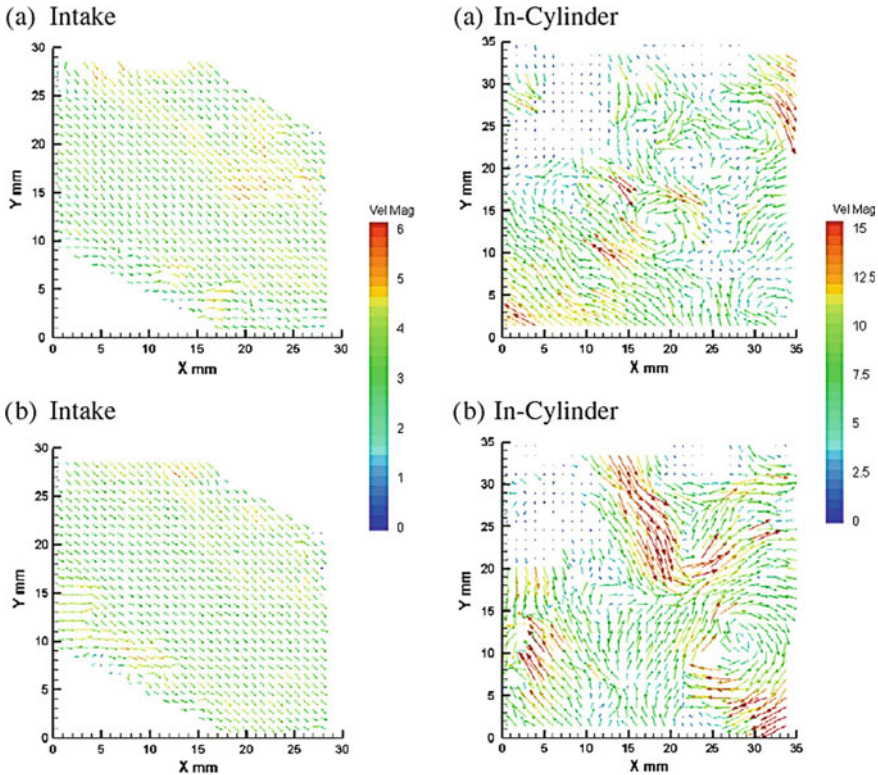


Fig. 7 Comparison of intake runner flow structure with in-cylinder flows [44]

despite of similar intake runner flows, in-cylinder flow is considerably different, leading to cyclic variations.

Piston geometry also has a significant impact on the flow patterns in the compression stroke. PIV enables complete visualization of these flow patterns and their effects on engine combustion. Deslandes et al. [21] studied the in-cylinder aerodynamics of a diesel engine using planar PIV in a transparent single cylinder engine for two different piston configurations; bowl-in-piston and flat piston in the intake and compression strokes. In the intake stroke, the intake jet flow and cylinder walls produce large flow structures, which hit the piston to form small structures. Their results showed that the bowl-in-piston has centered swirl however it remained unsymmetrical. It was also observed that the experimentally obtained squish intensity was relatively weaker than the theoretical expectations.

It is also possible to study the fuel spray-air flow interaction using PIV. Sasaki et al. [76] studied the flow-field near non-evaporating diesel spray using PIV. They reported temporal variation of air flow around pattern the fuel spray, using PIV auto-correlation technique. It was observed that the fuel-air interference leads to a complicated spray surface. Major finding of this research was that the air flow ahead

of spray tip has very low velocity compared to droplet velocity and the fuel-air interaction mainly happens in the mid-spray region and at the spray tip. Researchers observed that for detailed analysis of fuel-air interaction, detailed information about 3-D flow-field is required. Therefore different flow visualization techniques have been implemented to fully develop the complex 3-D flow patterns inside the engine cylinder. Implementation of planar PIV in different in-cylinder planes has emerged as an extensively used method for understanding 3-D flow structures. Dannemann et al. [18] implemented the planar PIV in different in-cylinder vertical planes to visualize 3-D flow-field evolution (Fig. 8). They analyzed the flow by studying the turbulent kinetic energy (TKE) and vorticity at 1500 rpm engine speed. Their results showed that the maximum TKE and its spatial variance decreased with increasing crank angle. Observations of in-cylinder flow-field suggest the existence of 3-D flow-fields, which call for the use of 3-D measurement techniques such as holographic and TPIV to completely analyze the in-cylinder flows.

Choi et al. [16] validated STAR-CD CFD code model by analyzing the in-cylinder flows using planar PIV measurements of a single cylinder diesel engine. The flow-field was visualized in the compression stroke at 600 rpm to show the streamlines, generation and the disappearance of tumble and squish. The study reported the difference of $\sim 26\%$ between experimental PIV and CFD results. For CFD code, both standard Reynolds k-e and RNG k-e turbulence model were used and it was shown that the standard Reynolds k-e model is more suitable for low engine speeds. In a similar study, Das and Chmiel [19] validated KIVA-3V code for in-cylinder flows in a GDI engine using the PIV technique. Experiments to study the flow-field were performed by PIV, while the computational study was done using RNG K-e turbulence model in KIVA-3V multi-dimensional code. Three planes of flow-field were analyzed by PIV; center plane, valve plane and swirl plane at 90° , 180° , 270° CAD aTDC. Results showed that the intake generated tumble motion weakened with a downward motion of the piston during the intake stroke and this tumble motion was enhanced with upward motion of the piston in the compression stroke. The discrepancies observed in the results of KIVA-3V code and PIV experiments were attributed to uneven valve seat surface.

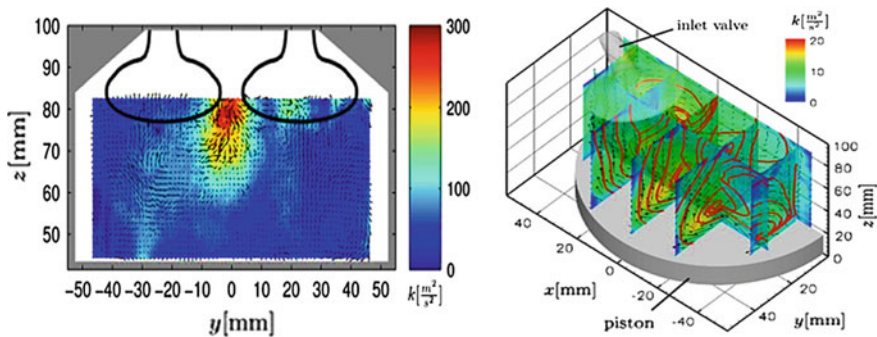


Fig. 8 2-D and 3-D TKE at 80° and 240° aTDC respectively [18]

Despite visualizing the flow evolution in different planes inside the engine cylinder, complete 3-D flow behavior cannot be fully understood till the volumetric flow-field is captured. Measurement techniques such as holographic PIV and TPIV enable complete visualization of the 3-D flow behavior. Baum et al. [10, 11] were one of the first researchers, who applied TPIV in IC engines. They investigated the 3-D flow-field of direct injection spark ignition (DISI) engines using TPIV. They used the principle of conservation of mass to address the uncertainty in 3-D velocity measurement and found the precision of 9% in the measured velocity data. This precision of velocity measurement is of the same order as volumetric flow measurement in a generic configuration indicating applicability of TPIV in IC engines. The flow-field analysis of the intake and compression stroke showed tumble formation and the velocity reduction from intake to compression (Fig. 9). The fluctuations in out-of-plane velocity component were analyzed by comparing the 2-D and 3-D TKE. Their results of 3-D-TKE at different crank angle positions showed the turbulence dissipation due to flow-cylinder wall interaction. Obtained flow-field was further analyzed by the Zentgraf et al. [97]. They studied the in-cylinder turbulence by analyzing the Reynolds-stress gradient tensor and anisotropic invariant tensor with homogeneous and isotropic turbulence as a reference. Because of the good agreement of RSGT data from TPIV and PIV, the authors were able to investigate the flow-field for larger field of view using planar PIV.

During the compression stroke near TDC, flow was affected by upward piston motion, leading to inhomogeneous turbulence. They reported that apart from crank angle position and engine speed, the flows also varied with their spatial position inside the cylinder. During the intake stroke, flow recirculation zone was approximated by isotropic turbulence levels, while intake-jet was approximated as anisotropic contraction and flow of the stagnation zone approximated as anisotropic expansion. These TPIV flow-field results were also used by Baum et al. [9] to validate the large eddy simulations developed for in-cylinder flows. Recently Singh et al. [80] applied TPIV for in-cylinder flow characteristics of an engine operated at different engine speeds, intake air temperatures and intake valve deactivation. The photograph of the experimental setup is shown in Fig. 10.

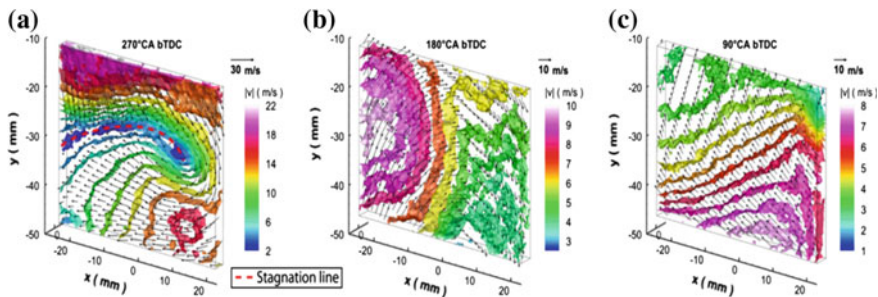


Fig. 9 Velocity iso-surfaces at 270°, 180° and 90° bTDC at 800 rpm [10, 11]

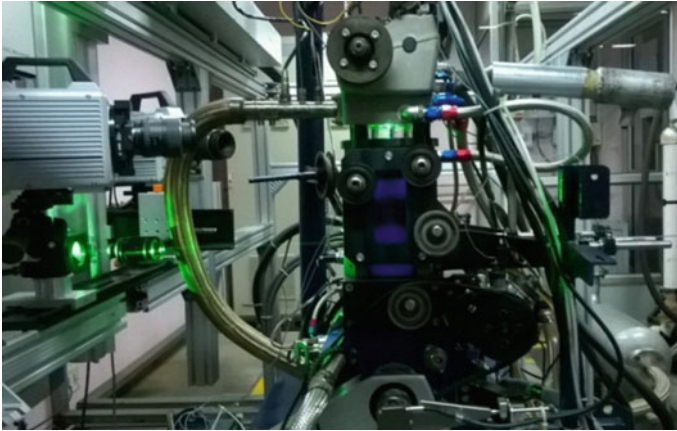


Fig. 10 Experimental setup for TPIV [80]

They reported that high velocities generated in the first half of the intake stroke started to dissipate in later stages of the intake stroke. A large part of flow energy of the intake stroke dissipated during the compression stroke. Therefore in the compression stroke, the flow became more homogeneous except locations near to the cylinder head. A higher rate of energy dissipation and velocity fluctuations were present in the intake stroke compared to the compression stroke. Higher piston speed and volumetric efficiency at higher engine speeds led to increased intake jet velocity and turbulence.

In another study by Singh et al. [81], flow evolution was investigated at different crank angle positions. They used TPIV and analyzed the flow behavior at different locations inside the combustion chamber. They concluded that flow behavior and different components of velocity were significantly affected by in-cylinder location. In similar study, Singh et al. [81] also investigated the effect of different intake port configurations, namely swirl port open and tangential port open configurations. They reported that swirl port open configuration provided highest average air velocity and vorticity, followed by both port open configuration. Tangential port configuration showed the highest rate of energy dissipation, which resulted in minimum absolute air velocity (Fig. 11).

3 Spray Characterization

Understanding fuel spray characteristics is very important for combustion in IC engines because it is an interface between fuel injection and combustion. It plays a very important role in fuel distribution, which directly affects fuel-air mixing. The main aim of spray investigation is to control the fuel injection system, and to deliver

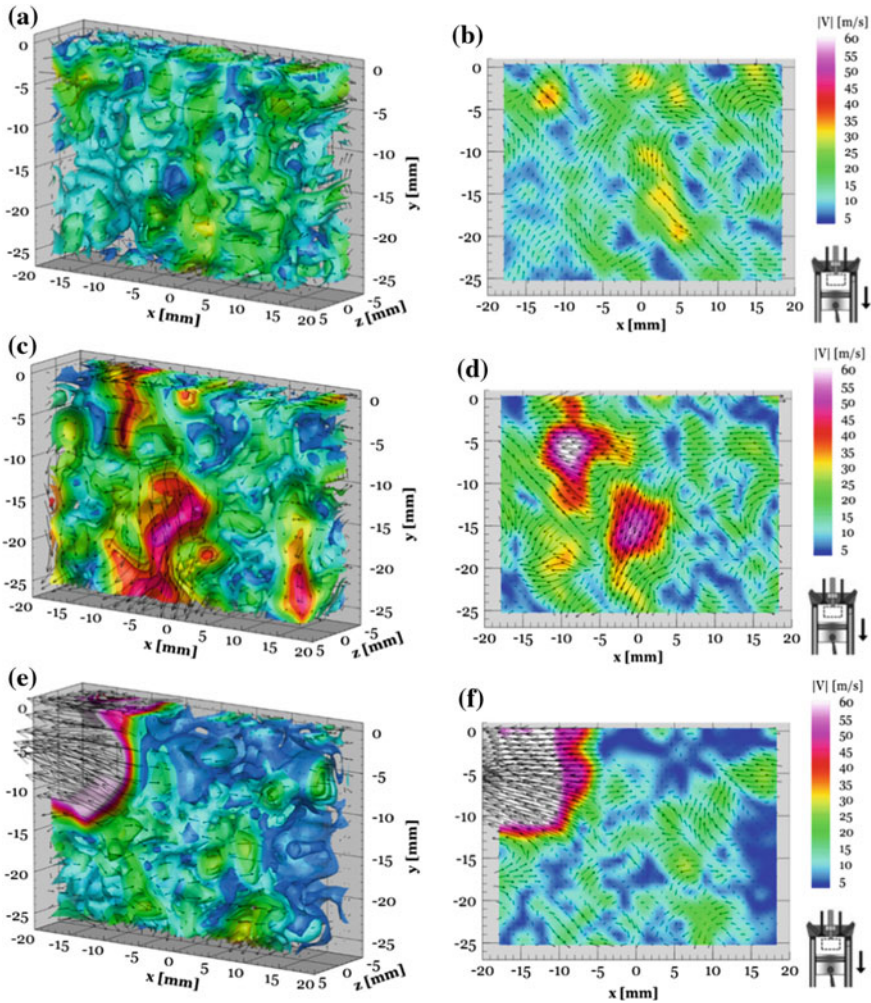


Fig. 11 Ensemble velocity profile at mid-intake stroke at 1500 rpm using different port configuration as **a** and **b** both ports open; **c** and **d** swirl port open; **e** and **f** tangential port open [80]

precise fuel quantity for obtaining optimal engine performance and lower engine exhaust emissions. Fuel-air mixing and auto-ignition of the charge is highly dependent on spray formation process starting from start of injection (SoI) to full spray development. Spray development after fuel injection and fuel cut-off is very critical for formation of different pollutant species during combustion. The spray formed due to pressure difference between the spray holes of the injector nozzle and ambient. After leaving the nozzle, spray jet becomes turbulent and partially mix with the soundings air. It flows away from the nozzle and the spray velocity

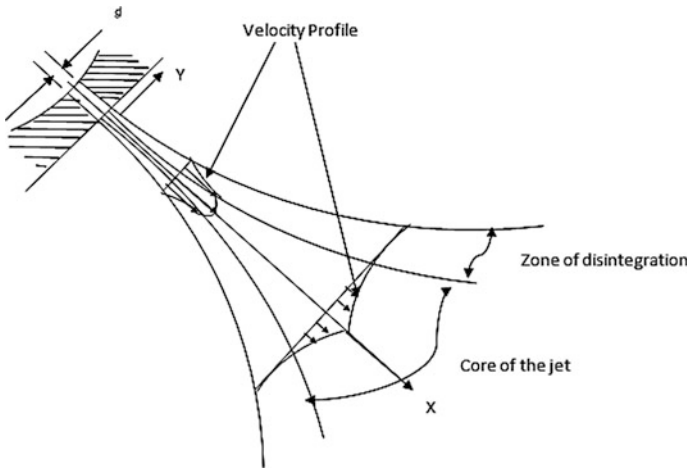


Fig. 12 Formation of fuel spray from a single hole [33]

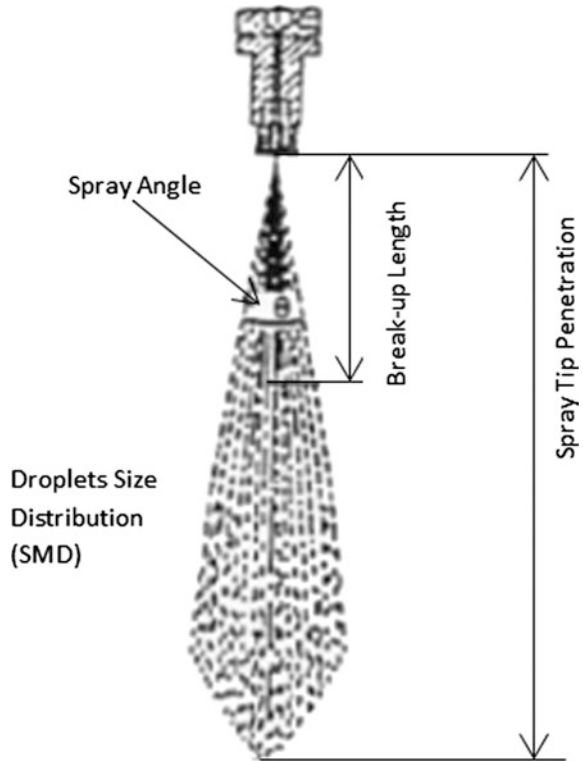
increases in X-direction. At the same time, it also spreads in Y-direction, which reduces the jet velocity in X-direction due to momentum conservation. In the X-direction, jet velocity further decreases due to frictional drag forces [35, 36]. Hence the fuel spray structure can be controlled by optimizing various microscopic and macroscopic parameters and spray atomization characteristics. In an engine, these characteristics can easily be determined using optical visualization technique such as endoscope however it needs high intensity lighting arrangement. Endoscopes are especially designed for low light applications. They are coupled with an optical fiber to illuminate the chamber during spray imaging. Using image analysis methods, these characteristics can be determined and compared for different operating conditions (Fig. 12).

3.1 Macroscopic Spray Characterization

Macroscopic spray characteristics consist of several geometrical spray parameters, which control the shape of the spray and help in optimizing the spray development process. In spray images, geometrical parameter can be measured by image analysis and can be optimized by varying fuel injection parameters. These parameters are as follows (Fig. 13).

- Spray breakup length
- Spray tip penetration
- Spray cone angle
- Spray area

Fig. 13 Spray parameters
[39]



Spray Breakup Length

It is defined as the length of the spray from the nozzle tip to point of discontinuity, where spray changes from dense packed zone of bulk liquid to finely atomized droplets. These droplets move in surrounding air so they have some relative velocity. This develops into non-uniform pressure wave, which further breaks the droplets into smaller droplets due to deformation. The detachment of liquid core to larger droplet is primary breakup and its further breaks up into smaller droplets is called secondary breakup [43]. Therefore, droplet density is the highest at the spray breakup point. These small droplets of liquid fuel reflect the illuminating light, while capturing the images. Hence higher density of droplets reflects higher illumination light rays. Therefore in spray images, breakup length can be measured as a distance from the nozzle tip to the maximum intensity point along the middle line of the spray (Fig. 14).

Spray Tip Penetration

Spray tip penetration (S) is defined as the maximum length from the nozzle tip to spray tip at a given time. In spray images, this length can easily be measured and

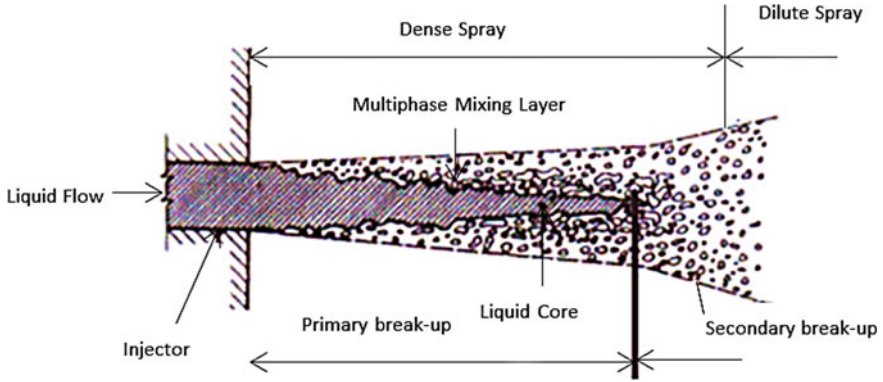


Fig. 14 Flow pattern of atomized spray [26]

multiplied by camera magnification factor. Spray length should be optimized for efficient combustion and pollutant formation. If spray length is too short, it results in poor combustion. If it is too long, it can hit the combustion chamber walls, which leads to fuel wastage and encourages soot formation. Spray length is significantly affected by FIP. Dent [20] derived the equation, which is based on jet gas theory and states that spray tip penetration increases with fuel injection pressure.

$$S = 3.07 \left(\frac{\Delta p}{\rho_g} \right)^{1/4} (td_n)^{1/2} \left(\frac{294}{T_g} \right)^{1/4} \quad (1)$$

Here, Δp is the pressure difference between the injection and ambient conditions, ρ_g denotes the ambient gas density, t represents the transmit time, d_n is the projection diameter and $(295/T_g)^{1/4}$ represents additional factor imposed on the relationship for accurate results.

Hiroyasu and Arai [39] measured spray penetration length with the help of photographic technique and correlated their data as mentioned below;

$$t < t_{break} \quad S = 3.07 \left(\frac{\Delta p}{\rho_g} \right)^{1/4} (td_n)^{1/2} \left(\frac{294}{T_g} \right)^{1/4} \quad (2)$$

$$t > t_{break} \quad S = 2.95 \left(\frac{\Delta p}{\rho_g} \right)^{1/4} (d_n t)^{1/2} \quad (3)$$

where $t_{break} = \frac{29\rho_d d_n}{(\rho_g \Delta p)^{1/2}}$.

Spray Cone Angle

Lefebvre et al. [53] suggested the definition of Spray cone angle as the angle between lines drawn from the nozzle tip to the outer periphery of spray at the downstream of the nozzle. It can be calculated from Eq. (4)

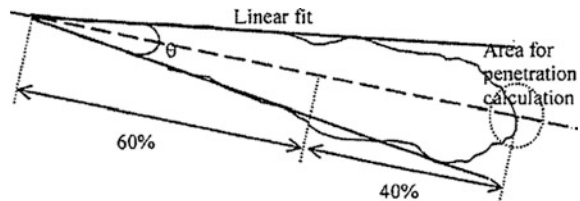
$$\tan \frac{\theta}{2} = \frac{1}{A} 4\pi \left(\frac{\rho_g}{\rho_l} \right)^{1/2} \frac{\sqrt{3}}{6} \quad (4)$$

Spray angle can be determined from spray images using linear regression method. Firstly spray contours are plotted on the basis of spray images and linear regression method is used for finding the upper and lower limiting lines, where intensity is rapidly reduced. Only point between injector and 60% of the total length is considered for applying linear regression (Fig. 15). The angle between these two lines is considered as spray cone angle [66].

Above mentioned parameters affect the overall spray behavior, which in-turn influences vaporization of fuel droplets and mixing of fuel and air inside the chamber. The emissions can be minimized and the efficiency and power output from an engine can be enhanced considerably, if spray can be optimized. Spray visualization can be done in a spray chamber as well as in an engine cylinder using a high-speed camera synchronized with a high speed laser and white light source for obtaining transient liquid droplet evolution for a complete injection. Spray penetration length and cone angle in a cold non-reacting environment using a common-rail direct injection (CRDI) system was first studied by Postrioti and Grimaldi [68]. Both experimental and numerical analysis of microscopic and macroscopic spray parameters using a common rail in a diesel engine was performed by Lee and Park [50]. They used particle motion analysis system to determine the spray tip penetration and spray cone angle, while the phase Doppler particle analyzer (PDPA) was used to study droplet's Sauter mean diameter (SMD) and axial velocity. They varied the axial distance between injector tip and measurement point and reported that as the axial distance increased from 10 to 30 mm, SMD and axial velocity of droplets decreased rapidly. On further moving downwards to 40 mm, these parameters almost remained constant. The reason was that as the spray formation zone was separated from the spray atomization zone, their rates became equal.

Many researchers have reported that all fuels exhibit longer spray penetration, wider cone angle and better fuel atomization at higher FIPs. Park et al. [62] studied

Fig. 15 Measurement of spray cone angle [66]



the effect of FIP on macroscopic spray parameters using a CRDI system. Increasing FIP resulted in longer spray penetration for both mineral diesel as well as biodiesel. The results were also supported by Suh et al. [89]. Wang et al. [94] investigated the effect of FIP on a spray cone angle and spray penetration length for mineral diesel. They reported that spray penetration length increased with increasing FIP and spray cone angle decreased. The effect of fuel properties on the spray characteristics and atomization was first studied by Lefebvre [53]. Abiola et al. [1] studied these parameters using mineral diesel and biodiesel in evaporating and non-evaporating environments. They reported that at very high FIPs, mineral diesel showed relatively shorter spray penetration compared to biodiesel. This was attributed to the higher volatility of mineral diesel, which resulted in higher evaporation compared to biodiesel, irrespective of FIP.

Biodiesel showed poor atomization characteristics compared to mineral diesel. Spray tip penetration and SMD were marginally higher for biodiesel, while spray dispersion and spray cone angle were relatively lower. Higher liquid length of biodiesel spray was attributed to its higher boiling range and higher heat of vaporization [174]. He et al. [38] analyzed the shape of biodiesel spray compared to mineral diesel. They reported that the spray tip penetration and spray cone angle of biodiesel were larger than baseline mineral diesel because of higher density, viscosity, surface tension and bulk modulus of biodiesel. Kim et al. [47] used two test fuels (biodiesel and DME) to study the spray characteristics in a constant volume spray chamber (CVCS). Suh et al. [89] compared fuel spray behavior on the basis of injection rate, spray penetration length, spray droplet-size distribution and axial velocity distribution for mineral diesel and biodiesel. Ejim et al. [24] and Abiola et al. [1] suggested that biodiesel had inferior volatility characteristics compared to mineral diesel, which resulted in inferior spray atomization. Therefore in order to improve fuel injection and atomization characteristics of low volatility fuels, they are blended with fuels having higher volatility.

Suh et al. [89] reported that blending ratio of biodiesel had an insignificant effect on their spray characteristics. Development of spray in case of mineral diesel was more advanced than biodiesel because of lower shear resistance offered by mineral diesel in the injector nozzle. Properties such as viscosity, bulk modulus, density and surface tension played an important role in providing shear resistance. Spray penetration length was also observed to be the same with or without considering the blending ratio. Gao et al. [29] investigated the reasons for reduction in spray cone angle with increasing biodiesel blending ratio. They reported that variation in spray cone angle showed local maxima, in which spray cone angle first increased with increasing biodiesel blending ratio and then decreased with further increase in biodiesel blending ratio. They explained this behavior as diffusion of smaller droplets, which resulted in narrower spray cone angle. Park et al. [64] concluded that the size of spray droplets decreased with increasing biodiesel blending ratio. It was found that gasoline blended with mineral diesel showed relatively smaller droplet sizes than baseline mineral diesel hence it can be used for improving the spray characteristics.

Researchers also investigated fuel spray characteristics using experimental and numerical techniques to correlate their findings. They concluded that fuel atomization and spray characteristics were two important aspects, which need to be improved in order to enhance in-cylinder fuel-air mixture homogeneity. As the spray droplet velocity distribution and the ambient air density increased, aerodynamic and viscous effects became more dominant and the spray breakup process became more complex. Small droplets offered larger surface area, enabling higher heat transfer and energy interactions compared to larger droplets for the same amount and volume of fuel injected.

3.2 Microscopic Spray Characterization

Microscopic analysis of spray indicates the spray droplet-size distribution, three velocity components, number density, time of arrival of droplets, and volume flux measurements. Laser Doppler velocimetry (LDV) or laser Doppler anemometry (LDA) techniques are used for microscopic spray analysis. These techniques measure the velocity of spray droplets however they do not give information about the spray droplet-size distribution. Therefore, these are substituted by phase Doppler interferometry (PDI). PDI technique, formerly known as phase Doppler particle analysis (PDPA) was developed by Dr. William Bachalo and Mike Houser in 1984. The principle of LDV is same as that of PDI. Phase Doppler interferometry is used to understand the intricate spray behavior in various fields such as in the turbulence generated by different flow regimes, high pressure injectors used in rockets, unsteady spray characterization in gasoline engines and compression ignition engines. PDI is a non-intrusive technique, which simultaneously measures the size and velocity of individual spherical spray droplets in inconsistent shapes, sizes and mass distributed flow environment. This technique is based on the principle of light scattering interferometry, which takes into account the wavelength of light. Since the intensity of light does not play an important role in measurement, thereby distorted light intensity has negligible effect on the performance of droplet-size determination. Parameters such as wavelength of the laser, focal length of the transmitter and receiver lenses, and detector separation are taken into consideration. Since the signals produced by the system are sinusoidal in nature, they are easily perceived even in presence of noise using Fast Fourier Transform (FFT). The schematic of basic PDI system is shown in the Fig. 16.

In PDI system, the laser is bifurcated into two beams of equal intensities using Bragg's cell and a beam splitter. The beams are then concentrated using a transmitter lens. Bragg's cell is used to shift the frequency of beams so as to provide exactness to the droplet direction. The laser, beam splitter and transmitter lens constitute a complete transmitter module. Two diodes pumped solid state lasers (DPSS) are kept inside the transmitter module, which have wavelengths of 532 nm

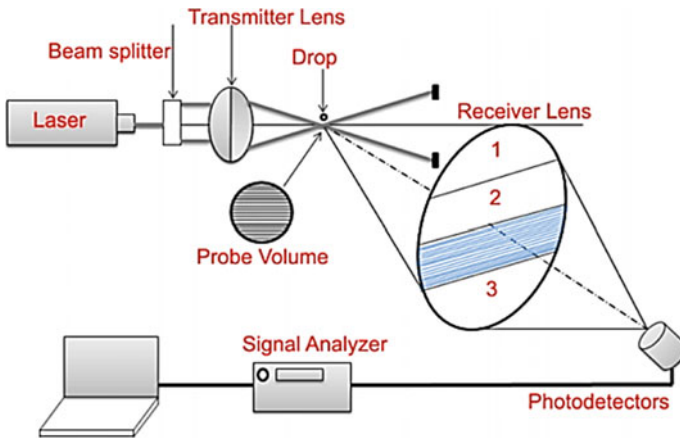


Fig. 16 Schematic of PDI system [54]

(green beam) and 471 nm (blue beam). Three photo-detectors, photomultiplier tubes and receiver lenses constitute a complete receiver module.

Spray droplets, while passing through the intersection point of the laser beams scatter light (refraction/ reflection), which is received by the photo-detectors of the receiver module through the receiver lenses. A single aperture is used to focus the refracted light from the receiver lens to the photo-detectors. A spherical spray droplet at the intersection of two laser beams (with enlarged view) is shown in Fig. 17.

As a result, an interference pattern is formed around the droplet. This interference pattern produces signals of sinusoidal intensity distribution, which when projected onto a plane gives hyperbolic signals. Once the separation between the detectors (s) is known, the spatial wavelength (Λ) and phase shift (ϕ) is calculated, which is helpful in finding the droplet size.

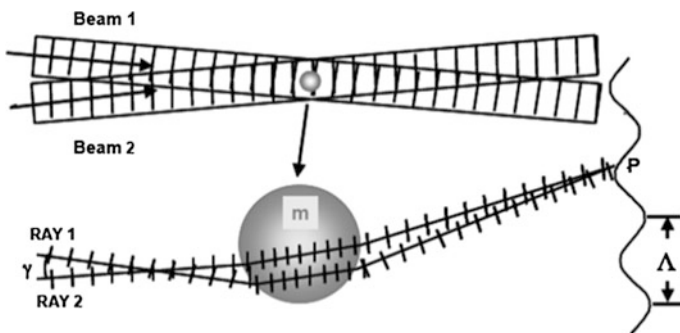


Fig. 17 Phase shift by two beams of light to reach a common point [54]

3.3 *Application of Spray Parameters in IC Engines*

The homogeneity in fuel-air mixing and combustion process inside the engine cylinder, reduction in emissions, and enhancement in the engine performance are some of the compelling reasons to study the spray formation, spray breakup and atomization in an engine. Thermal efficiency and power output of an engine can be increased by optimizing spray parameters. Physical and thermal properties of test fuels such as kinematic viscosity, bulk modulus of compressibility, volatility, surface tension, rate of vaporization, boiling temperature, etc. and ambient gas density play a prominent role in spray formation and fuel-air mixture formation. Apart from these properties, cavitation inside the injector nozzle and turbulence at the exit of the injector nozzle tip are also very important, which need to be looked for complete study of spray behavior. To investigate this, apart from an experimental perspective, theoretical and numerical approach has been adopted by a large number of researchers [47, 50, 62, 74]. Most of the experimental investigations are carried out in reacting or non-reacting environment in a specially built spray chamber. This CVSC is designed and developed in such a manner that it should create actual engine combustion chamber conditions except temperature and turbulence. Once the spray is analyzed for a particular injector nozzle type, the design of the nozzle geometry can be ameliorated. Hence the basic spray behavior is determined by the injector nozzle design. The study of fuel sprays behavior for diesel, vis-à-vis vegetable oils, biodiesel and blends in simulated compression ignition engine conditions needs to be thoroughly investigated. The fuel is introduced by an injector nozzle by creating a pressure difference between the ambient and the fuel injector. Generally, the ambient pressure and the FIP inside the combustion chamber were kept in the range of 1–60 bar and from 150 to 2000 bar respectively. This range depends on the size of the engine and the fuel injection system used. Combustion in a CI engine is highly dependent on the quality of spray and atomization during the fuel injection. A good spray should ensure that the injected fuel jet enters into the combustion chamber at sufficiently high velocity and consequently atomizes into small droplets to enable rapid vaporization and mixing with ambient air and form combustible mixture. When mineral diesel is replaced by biodiesel, it is essential to optimize the fuel injection system for the new test fuel. Different straight vegetable oils (SVOs), biodiesels and their blends with mineral diesel have significantly different physical properties, depending on the chemical structure of the biodiesel feedstock. Because of higher viscosity, surface tension and density, biodiesel and their blends exhibit inferior spray characteristics hence poor air-fuel mixing. Liquid fuel distribution visualization in an engine cylinder or a constant volume spray chamber provides useful information on the evolution of spray, spray penetration, spray cone angle, spray-wall interaction and spray area. These parameters depend on fuel droplet dispersion, axial and radial velocity distributions, number density, and volume flux measurements. Study of these factors in a gasoline or diesel engine combustion chamber makes the task extremely

chaotic and challenging. Therefore so far no research has been reported in the open literature, which investigates these parameters inside a firing engine. All reported research is carried out in a CVSC only.

For measuring droplet size and spray velocities, Kim and Lee [46] and Koh et al. [49] used image processing methods. However, this method does not provide complete information because it was very difficult to study coalescing droplets. Schunemann et al. [79]; Park and Lee [65] and Lee and Reitz [51] used PDPA technique for studying spray atomization. Most researchers investigated different alternative fuels and adopted various visualization and quantitative methods to study spray behavior. Kim et al. [47] used two fuels, namely biodiesel and DME to study the sprays in a CVSC and varied the FIP and ambient pressure. The injection system used in this study consisted of a common rail and a high pressure pump. They also varied the axial and radial distance of the injector tip from the central axis of the measurement point and studied the spray characteristics at different locations. They reported that with increasing axial distance in the downstream direction, SMD of biodiesel droplets increased, however SMD of DME remained almost constant. The reason stated was that DME, due to its lower viscosity and density, atomizes very early. Hence the spray formation and atomization zones occur in the very early stage for DME and this leads to constant SMD droplets throughout the measurement volume. The spray images obtained by the high speed camera were converted to cell-images using image processing technique. This technique is called 'threshold method'. To differentiate between the dark (black) and bright (white) spray pixels, the values of light intensity were selected from 0 to 255. Here 0 indicates that the pixel has a brightness level of 0 grayscale or a darkness level of 256 gray scales and 255 indicates vice versa. The spray area is defined by the sum of the total number of pixels selected. They reported that because of adequate atomization in the extreme region of the spray, light intensity levels were lower. However in the central region of the spray, light intensity was higher.

Ghurri et al. [30] used image posterization processing method instead of the threshold method. According to them, posterization method gives more detailed information about the spray because it divides a complete image in layers of various gray level scales. Segmentation of image processing technique is generally employed to separate the captured images and the spray background. The threshold method of image processing transfigures gray images (as captured by the camera) into shades of pure black and pure white. In order to differentiate between black and white images, a threshold value is selected such that if the image is brighter than this value, it will be referred to as a white image otherwise it will be referred to as a black image. This lengthy procedure of segmentation has to be applied to each image. This problem was rectified by posterization image processing method, in which a threshold value was applied to a single image and on the basis of that value, other images were interrogated. Gao et al. [29] simulated the biodiesel sprays using Star-CD software. The simulations obtained were in good agreement with the experimental data. Galle et al. [28] used shadowgraphy technique to capture the

spray images with the help of a high speed camera. Sakaguchi et al. [74] measured the droplet sizes of diesel spray with the help of laser-2-focus (L_2F) velocimetry technique, in which there were two focal points of the probe and the distance between them was 36 μm . To increase the data rate and to improve the accuracy, multiple scattering of the particles are circumvented. This L_2F technique was first introduced by Schodl [78]. In order to calculate the flow measurement and to increase the signal-to-noise ratio in the impeller of a centrifugal compressor, L_2F technique was used. The work of Schodl [78] was further advanced by Chaves et al. [15]. They used L_2F technique in engines for measuring the diesel spray droplets, in which, the distance between the two focal points was 60 μm . The diameter of the probe focus was 10 μm . Kuti et al. (2013) studied the effect of Mie-scattering in reacting spray environment and the effect of OH Chemiluminescence on the flame lift-off length.

An important contribution to the field of spray structure was made by Park et al. [62]. They studied the effect of fuel temperature and back pressure on the spray behavior in a diesel engine. The fuel used in this study was diesel and soybean oil methyl ester (SOME). The experimental results using PDPA were compared with numerical simulation results obtained using KIVA-3 code. The parameters tested were local and overall SMD at a variable distance from the nozzle tip. The spray breakup models used for the primary and secondary breakup were Kelvin-Helmholtz (KH) and Rayleigh-Taylor (RT) models. A computational model for studying the spray behavior and injector characteristics for different fuels (diesel and biodiesel) was developed by Som et al. [82]. Parameters such as cavitation and turbulence at the nozzle outlet were studied using simulations. In order to ensure that the efficiency of the fuel injected is the maximum, they investigated various injection pressures and back pressure conditions in a diesel engine. CONVERGE software based on Kelvin Helmholtz-Aerodynamics Cavitation Turbulence (KH-ACT) model was used to completely understand the spray behavior and spray characterization inside the engine combustion chamber. They compared the results of this model with KH-RT model and reported that spray penetration of biodiesel was longer than diesel using KH-ACT model. Due to turbulence and cavitation, apart from lower fuel viscosity and surface tension, atomization of biodiesel spray was faster, which resulted in a smaller spray droplets-size distribution and smaller penetration length compared to diesel. Since KH-RT model does not take into consideration the effect of turbulence and cavity, the results showed the opposite trend. Park et al. [63] also investigated the effect of multiple fuel injection strategy in reacting and non-reacting environment in a diesel engine and used spray visualization and PDPA techniques. Elkotb [25] developed a relationship for determination of SMD of a single phase flow using fuel properties like viscosity, surface tension, pressure difference and density. Ejim et al. [24] verified that this relationship can be applied to dense diesel and biodiesel sprays. This relationship is given as:

$$SMD = 6156\nu^{0.385} \sigma^{0.737} \delta_f^{0.737} \delta_a^{0.06} \Delta P^{-0.54}$$

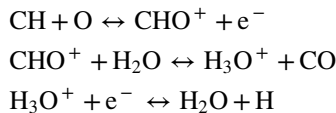
Here ν and σ are viscosity and surface tension, and ΔP is the difference in fuel injection pressure and ambient pressure. It is to be noted that SMD, ν , σ , δ and ΔP have units of μm , m^2/s , N/m , kg/m^3 and bar respectively.

4 Combustion Diagnostic Techniques

Strict emission legislations and fuel economy compliances are very important for the automotive industry. They can be controlled by analysis of different combustion and spray parameters, which can be used to optimize engine design and fuel injection parameters. Combustion and sprays can be diagnosed by several techniques. There are several classical techniques such as optical detectors (Photodiodes, Photo multiplier tubes), and mechanical sampling methods, which are of no interest to the engine researchers, hence these are not covered in this chapter. Ion current probe method, spectroscopy, optical sensors, optical particle sizing methods and optical visualization technique are some of the advanced techniques, which are currently used for combustion and spray diagnostics by the automotive industry and researchers. These techniques are briefly discussed in following sub-sections.

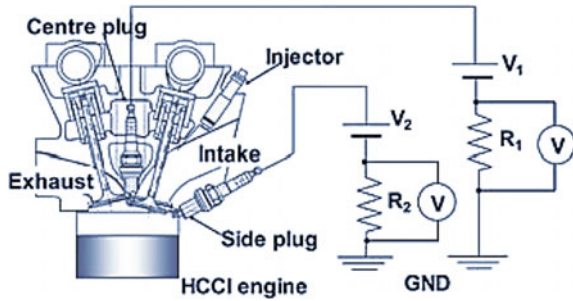
4.1 Ion Current Probe Method

It is based on electrical characteristics of combustion reaction. Docquier and Candel [23] suggested that the main source of ions in flames is chemi-ionization process, which occurs, when the energy of reactants together with reaction energy is large enough to ionize the product. CHO^+ and H_3O^+ are the positive ions in the combustion flames, which are mainly responsible for ion current. The chemical reactions of generating ions are as follows:



These positive ions CHO^+ and H_3O^+ are mainly generated from CH, which originates from fuel. Ions are also generated by thermal reactions of NO, as shown by Zeldovich mechanism. This method is mainly used in SI engines. The spark plug is used as an Ion current probe. Tanaka et al. [92] used this method for combustion

Fig. 18 Schematic of the ion current detection circuit [92]



analysis of HCCI in SI engine. They used two spark plugs for detecting the Ion current; one was mounted in the center and the other was mounted near the wall. Their experimental setup and current detection circuit are shown in Fig. 18.

They detected ion current and pressure signal w.r.t. crank angle and found one peak on HCCI mode and more than one peak in normal SI mode. It clearly suggested absence of NO_x emissions in HCCI mode. They also found that starting timing of current signal is dependent on gas temperature, while the peak of current signal is influenced by the gas composition. Length of the peak was the maximum for stoichiometric mixture, which suggested that large number of ions were generated in stoichiometric mixture. This technique is good for SI engines, because spark plug works as a current probe and no extra arrangement is required, however in CI engines, it is very difficult to access probes in different locations of the combustion chamber.

4.2 Spectroscopy

It is used to determine combustion temperature and species emitted in combustion process. It measures the intensity of light spectrum emitted by combustion gases. Wavelengths of this spectrum lie in infrared, visible and ultraviolet regions. Combustion temperature can be determined according to Planks or Wine's Law and Kirchhoff law. Radiance is measured at a particular wavelength and temperature can be calculated according to Wien's law, which states that the maximum flux is attained at lower wavelengths upon increasing the temperature (Web 2009).

$$L_{\lambda}^b(T) = \frac{c_1}{\left\{ \pi \lambda^5 \left(e^{\frac{c_2}{\lambda T}} - 1 \right) \right\}}$$

λ = wavelength; c_1 , c_2 = radiation constants; $L_{\lambda}^b(T)$ = spectral radiance and T = Temperature.

4.3 Optical Sensors

Various types of optical sensors have been developed for determining emissions, presence of flames and temperature. These sensors are usually installed in the inlet and exhaust pipes. Gaseous emissions (NO_x , CO, etc.) are normally determined by semi-conductor sensors, which are made of metal oxides such as TiO_2 , ZrO_2 , and SnO_2 [23]. Working principle of TiO_2 and SnO_2 sensors is based on the change of semi-conductor resistance with partial pressure of oxygen, while in ZrO_2 sensors, the presence of species can be determined from the change in current and voltage. Apart from this, there are several other sensors like resistive temperature detectors, pressure sensors and flow sensors, etc., which are used for determining exhaust temperature and chamber pressure. Main problem with the optical sensor is that they each sensor has limited applications. Hence different types of sensors are required for different applications.

4.4 Fraunhofer Diffraction Method

This technique is typically used for spray analysis. When a beam of monochromatic light falls upon a large diameter droplet/ particle ($d \gg \lambda$), light is scattered and it forms Fraunhofer diffraction patterns [36]. Particle diameter is determined from the angular distribution of scattered light in the diffraction pattern. This technique is good for detecting large diameter droplets/ particles. Lafevre et al. (1989) found that there are inaccuracies, while measuring the particle less than $5 \mu\text{m}$ diameter. The major drawback of this technique is in dense sprays due to multiple scattering. It also does not work well for non-spherical particles (Fig. 19).

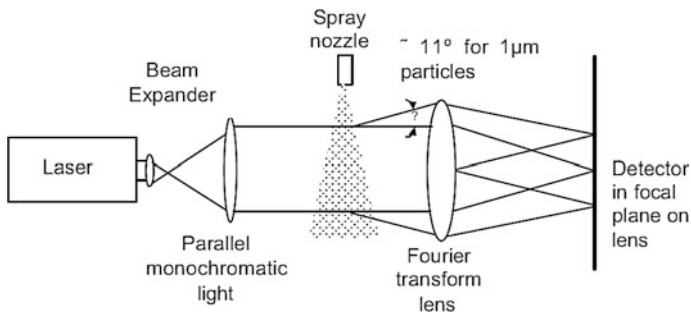


Fig. 19 Schematic of Fraunhofer diffraction technique employed in Malvern particle arrangement [77]

4.5 Laser Sheet Droplet Sizing

This technique is a combination of Mie scattering and LIF for calculating SMD of dense sprays. Laser sheet is used to measure the image cross-section of sprays and illuminate the droplets/ particles. A part of the energy is absorbed by these droplets/ particles, which excite and emit fluorescence. Remaining part of incident light is scattered and experienced by elastic light scattering. Intensity of scattered light signal from a droplet of diameter D_d is calculated using Lorenz Mie theory of elastic scattering;

$$S_{Mie} = C_{Mie}(D_d)^2$$

The droplet's molecules emit fluorescence signal, which is S_{LIF} .

$$S_{LIF} = C_{LIF}(D_d)^3$$

Ratio of fluorescence and Mie scattering signal from a large number of droplets is proportional to

$$\frac{S_{LIF}}{S_{Mie}} = \frac{C_{LIF}D_d^3}{C_{Mie}D_d^2} \propto \frac{D_d^3}{D_d^2} \text{ or } SMD$$

Hence SMD can be calculated by taking ratio of these two signals and its map in image plane can be generated by a ratio of two images and divided by the calibration constant. This technique works well in dense sprays, but it is limited to measuring only SMD. It also works with maximum diameter up to 20 μm [36].

4.6 Applications of Optical Diagnostics in Engines

Following combustion features can be determined using combustion visualization techniques:

- Combustion temperature,
- Start of combustion and ignition delay,
- Flame propagation and flame velocity in SI engines.

4.6.1 Combustion Temperature

Combustion in IC engines generates heat, and releases hot exhaust gases through the exhaust valve. Performance and emissions from an engine are directly related to in-cylinder temperature. In diesel engines, NO_x (which include NO and NO_2) is a major pollutant and its formation mainly depends on the peak combustion

temperature. NO, which is a toxic and colorless gas, is formed during oxidation of atmospheric nitrogen at high temperature (Zeldovich mechanism) in post-flame combustion processes [4]. NO₂ is formed during a reaction of NO with HOO⁻ radicals in combustion zone and it is converted back into NO by reacting with atomic oxygen. This NO₂ decomposition reaction freezes, when high temperature exhaust gas rapidly mixes with ambient air. Therefore, NO₂/NO concentration ratio was higher at lower engine loads due to higher probability of high temperature gas coming in contact with cold ambient air [36]. NO_x concentration is significantly lower in SI engines as compared to CI engines therefore it can be controlled by using catalytic devices. However in diesel engines, it is controlled by using EGR. Agarwal et al. [4] suggested that NO_x emission reduced in CI engine on increasing EGR, primarily due to reduction in peak combustion temperature in the cylinder. Hence the combustion temperature is very important combustion characteristics for controlling NO_x emissions. Optical visualization techniques such as engine endoscopy are very useful for finding the combustion temperature using combustion imaging and optical pyrometry. Normally 'ThermoVision' software with endoscope is used for finding the temperature during in-cylinder combustion however colour temperature methods are also helpful for comparing the combustion temperature distributions for different fuels.

4.6.2 Ignition Delay and Combustion Duration

Fuel after being injected from the nozzle undergoes physical and chemical processes before the ignition takes place. There is a delay between the start of injection and start of combustion, which is called 'ignition delay'. Physical delay part of ignition delay includes atomization, evaporation and mixing with air, while the chemical delay part of the ignition delay is due to pre-combustion reactions in the fuel-air mixture, which leads to auto-ignition. Mtui and Hill [58] suggested that ignition delay can be measured experimentally as time between start of injection and 10% mass burn fraction. It can also be found from the combustion images. Start of combustion can be easily found by visualizing the combustion chamber during combustion.

4.6.3 Flame Propagation and Flame Velocity in SI Engines

In SI engines, flame propagation is very important phase of combustion process because it directly affects the knocking in the engine. Higher flame propagation velocity reduces knocking combustion due to shorter flame propagation duration. Spicher et al. [84] visualized combustion process and reported that the flame propagates in unburned mixture in a spherical wave form with a wrinkled surface. Experiments were performed in a DISI engine with homogenous and stratified charge using an endoscope (Fig. 20).

Koch et al. [48] developed the phenomenological model in a DISI engine for calculating the flame front velocity with the help of optical experiments, which

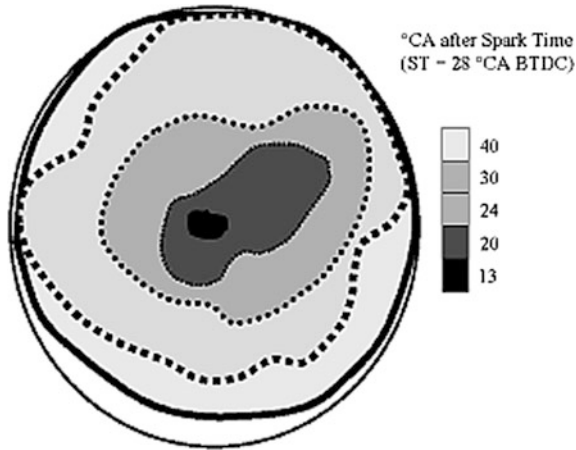


Fig. 20 Spherical flame-front in DISI engine with homogenous mode [86]

were performed on a single cylinder research engine. They captured the combustion images and analyzed flame propagation velocity, flame front area and suggested that air-fuel ratio changed with flame front propagation. Rhodes and Keck [70] as well as Metghalchi and Keck [56] suggested that the laminar flame speed mainly depends on the air-fuel ratio, temperature, pressure and mass burn fraction in a SI engine. In a diesel engine during pre-combustion phase, motion of gases affects the

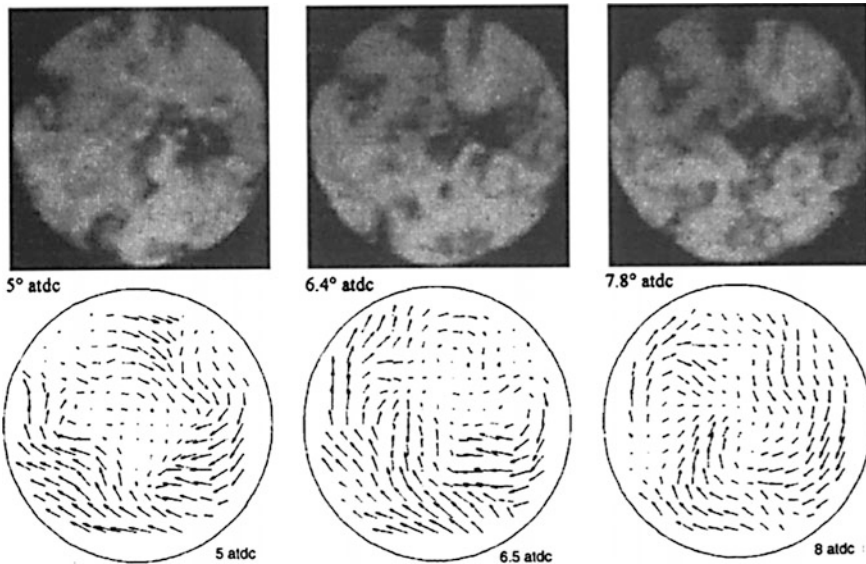


Fig. 21 Combustion images with velocity vector plot [90]

post-combustion processes. Sun et al. [90] measured the flow-field of gases using high speed combustion photography and cellular cross-correlation technique and analyzed its effect on the combustion processes (Fig. 21).

They plotted the velocity vector for different swirl ratios and found that with increasing swirl, flame velocity also increased and forced vortex dominated the flow in the combustion chamber.

5 Combustion Visualization

In IC engines, most emission and performance tests have been done passively and such investigations do not provide vital spatial and time resolved information about the formation of pollutants during combustion. It is possible only with direct visualization of combustion and sprays in the engine cylinder, which can be done by using sophisticated optical visualization techniques. Hence combustion and spray diagnostics in engines are very important because it is one of the most effective ways to understand and resolve the engine emission formation in the engine combustion chamber. In-cylinder combustion visualization can be carried out by using a high-speed CCD camera and associated visualization equipment in a customized engine. From these images, various combustion parameters and spray characteristics can be analyzed with the help of image processing software. However optical access to the engine combustion chamber is the biggest challenge in applying optical diagnostic techniques to engines. There are different ways of gaining optical access to the engine cylinder and it differs according to the requirements of the measurement and available financial resources. Two main types of optical access arrangements can be made namely; full optical access such as in an optical research engine; and limited optical access such as in engine endoscopy of a production grade engine.

5.1 *Optical Research Engine*

An optical research engine allows full optical access to the engine combustion chamber. This special engine is used for studying the fuel-air mixing, in-cylinder flows, combustion, and flame propagation through the optical liner, which is made of high quality quartz and a transparent piston. Early efforts on gaining optical access were by using a transparent acrylic resin, which was assembled on the extended part of the cylinder. A quartz window was installed on top of the extended piston, which enclosed a mirror inclined at 45° to observe the motion of in-cylinder flows. Bowditch [13] modified a production engine for optical access through the piston crown and developed it as a new tool for combustion research. After that, several researchers and automotive companies improved this type of engines and implemented this technique using a transparent window in strategic locations such

as cylinder, cylinder head and piston for investigations in engine firing conditions. Fully transparent cylinder was also implemented in some engines for non-firing studies. Transparent windows were made of fused silica or high temperature quartz, which is capable to withstand high temperature and high pressure prevailing during combustion. This type of engine is fired for very short periods only because the visibility of the optical window decreases rapidly due to soot deposition. Therefore, regular cleaning is required after each firing experiment. Optical engines cannot be tested at higher loads and speeds [36]. Allen et al. [6] used new design of the optical research engine, developed by Lotus Engineering, UK. Fuel spray and combustion investigations were done in this engine by employing laser diagnostics. They tested the engine up to 5000 rpm and 60 bar peak in-cylinder pressure. Han et al. [32] used optically accessible direct injection diesel engine for soot and temperature analysis using laser diagnostics. The main advantage of this engine was that entire combustion event could be captured for one full combustion cycle using suitable high-speed charge coupled device (CCD) camera. Hence this type of engine was very helpful in analyzing various combustion characteristics, which were not understood well using conventional techniques. Huang et al. [41] used a transparent cylinder, which was made of Plexiglas and a section of aluminum cylinder. A chrome metal liner was inserted between the Plexiglas cylinder and the crankcase. An elongated hollow cylindrical aluminum frame was used instead of the original piston. The top end of the cylindrical frame was screwed to the piston head. Richter et al. [72] used standard Bowditch layout, in which a quartz cylinder of 80 mm height was mounted to access the combustion chamber (Fig. 22a).

Singh et al. [80, 81] used an optical research engine (AVL, 5408) for PIV experiments in motored conditions. The engine had full optical access through the optical liner made of quartz and a transparent piston, in the Engine Research Laboratory of IIT Kanpur, India. Lotus single cylinder optical research engine (SCORE) was designed for optical diagnostics as well. Its cylinder liner was made from fused silica and a sapphire window was inserted in the piston crown in order to provide full optical access to the combustion chamber (Fig. 22c). Optical diagnostics using full optical access are very useful for real time data analysis however optical engines have several limitations. Optical research engines suffer from several restrictions such as balancing difficulty of a single cylinder, which is due to the added mass of the elongated piston. This type of engine can only be operated from low-to-medium loads and speeds because the limited structural strength of the optical window, which is a limiting factor due to its large size. Quartz window is very expensive and a specific window is required for a particular engine according to its geometrical configuration. Hence this technique can't be used in a production grade engine. It can only be used for research in a highly customized research engine test cell environment, which is prohibitively expensive. The optical engine can be operated for short durations only due to low heat transfer rates through the optical components and lack of cooling of the optical liner. The optical walls must be cleaned and combustion products must be removed frequently. This is quite tedious task generally.

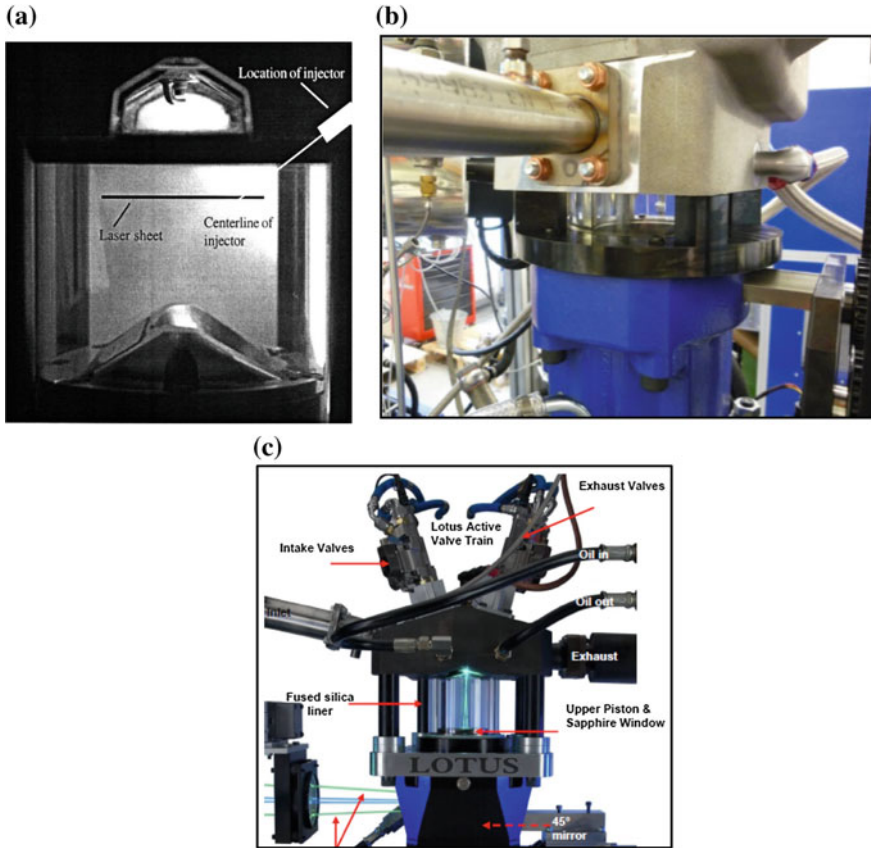


Fig. 22 **a** Optical access with 80 mm quartz liner [72]; **b** AVL single cylinder optical research engine [80]; **c** Lotus single cylinder optical research engine [12]

5.2 Engine Endoscopy

Due to the above mentioned limitations of optical engines, several optical diagnostics techniques use optical access using an endoscope, which is relatively easier and endoscopic technique can be applied to any production grade engine with some modifications in the engine hardware. Endoscopy is an optical visualization technique used for several medical and industrial applications. Initially this technique was used by doctors in medical surgeries for capturing the view of interior parts of the human body. It was used for the first time in 1806 by Philippbonzzini in Mainz using light conductor for examining the cavity in a human body. After many improvements in this technique, Georg Wolf (1873–1938) introduced rigid endoscopes in 1906 and flexible endoscope in 1911. At the time of World War-II, several modern technologies emerged in medical science. In 1945, Karl Storz, who is known

as “father of endoscopes” introduced a new endoscope, which was used with external light source in the human body. After that, this concept was widely used in industry for investigating problems which were associated with the interior part of machines in locations, where there is limited space for optical access. After that, it was designed for automotive applications for visual inspection of hollow spaces and areas, which are challenging for optical examinations such as engines, cylinder heads and intake manifolds of the engine. It can be used in myriads of applications in SI and CI engines, both for combustion diagnostics, spray formation, mixture formation etc.

5.2.1 Principle of Endoscopy

The endoscope is a large, thin tube, which consists of achromatic lens or rod lens combinations used for transferring image from the viewing end to the ocular (eye-piece). The image is transferred through image lenses and field lenses, which are set in the guide tube in alternate sequence. These pairs of lenses form an image reversal system, which repeats the reversal of image and transfers the image straight through the endoscope (Fig. 23).

The image of an object is first projected at plane B1 (Fig. 23) and from there, it is transferred through reversal lenses (L1/ L2) and projected on B2 plane. Image on plane B2 is a mirror image of plane B1. In the same way, it is transferred to Plane B3, where image is similar to image plane B1. C mount adapter is attached to the ocular, which consists of focus adjustment arrangement [22].

5.2.2 Methodology of Engine Endoscopy

Normally for engine applications, two types of endoscopy can be used: (i) combustion chamber endoscopy and (ii) general cavity endoscope. Combustion chamber endoscopy is used for high temperature and high pressure applications such as visualization of in-cylinder combustion process. This type of endoscope is

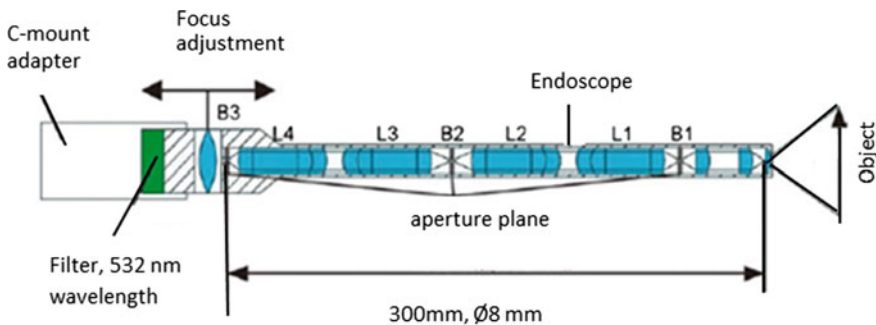


Fig. 23 Image transformation through an endoscope [22]

coupled with a cooling arrangement in order to protect it from high temperature and high pressure combustion gases. Normally combustion is captured in the absence of light because sufficient light is emitted by the soot formed in the combustion chamber however fuel spray needs to be illuminated by an external light source. Dry and dust-free air is circulated through the endoscope assembly at ~ 6 bar pressure to keep it cooler and to avoid its damage during the experiment. General cavity endoscopy is used in low temperature, low pressure conditions, where cooling is not required, e.g., visualization of mixture formation process in SI engines. Optical fiber is coupled to the lens system in the endoscope for transmission of light, which is used for illuminating the area of capturing the images.

Engine endoscopes gain access into the engine combustion chamber through the cylinder head. For combustion and spray diagnostics in an IC engine, a hole is made in the cylinder head such that its endoscopic view can capture the image of the illuminated area of interest and it covers a maximum possible view of the combustion and fuel spray. Schematic of the engine combustion chamber endoscopic access and its components are shown in Fig. 24.

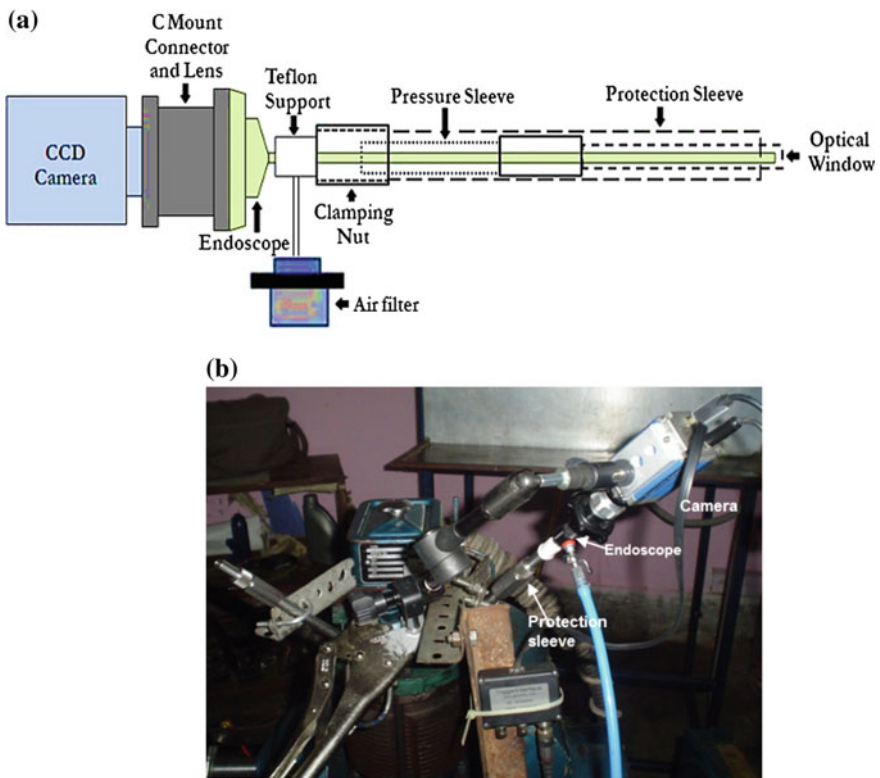


Fig. 24 Components of the engine endoscopy and its mounting on the engine: **a** schematic of the endoscopic access system, **b** common arrangement of engine endoscope with camera [2]

For a long time, endoscopic technique has been used to investigate the combustion process in CI engines. Different combustion and spray parameters have been determined in diesel engines using this technique. Further, it is combined with lasers to provide access to complex engine geometries and used for characterization of combustion and mixture formation in indirect and direct injection spark ignition engines. It was used for modifications of combustion chamber shapes for optimizing the fuel utilization and reducing soot formation. Recently it has been used in several advanced applications in automotive industry, which were otherwise very difficult for conventional techniques such as determining piston temperature, studying the pilot injection combustion of diesel and the effect of intake charge condition on the in-cylinder combustion temperature and soot distributions. Several researchers have used endoscopy in different areas of engine research in SI and CI engines.

5.2.3 Application of Engine Endoscopy in Engines

Several researchers have used the endoscopic technique to diagnose the effect of different engine parameters on combustion properties. Hampson and Reitz [31] investigated the advantages of double injection over single injection on combustion characteristics such as combustion temperature and soot distribution using endoscopic visualization technique. They captured combustion images in modern heavy-duty diesel engines equipped with common rail electronically-controlled, high-pressure fuel injection system, which could inject the fuel four times in one engine cycle. Combustion temperature and soot distribution were analyzed using a two-colour pyrometry technique. They also developed a multi-dimensional simulation model for verifying the data and got a good agreement between experimental and simulated results. They explained the reason for reducing soot with split injection and advancing the injection by endoscopic images in conjugation with modelling (Fig. 25).

A combustion phenomenon was also observed by Spicher et al. [86] in a DISI engine using endoscopy. They analyzed combustion characteristics such as flame propagation speed, and flame radiation and compared them in homogeneous and stratified combustion modes. Optical spark plug and endoscope were inserted in place of one outlet valve of a 4-valve engine. Flame fronts of combustion were captured at a difference of 0.2° CA and plotted in contours (Fig. 26).

Several studies were also conducted for comparing combustion characteristics of different alternative fuels with baseline diesel with the help of an endoscope. The endoscopy proved to be very helpful in such study because different real time characteristics were analyzed by changing different parameters of the engine and fuel injection system. Miers et al. [57] conducted a similar study with Sun-diesel, which is an alternative biodiesel derived from wood-chips. The endoscope was installed in Mercedes A-class engine, which was equipped with CRDI system. They analyzed soot concentration factor from combustion images for both fuels at different SoI timings.

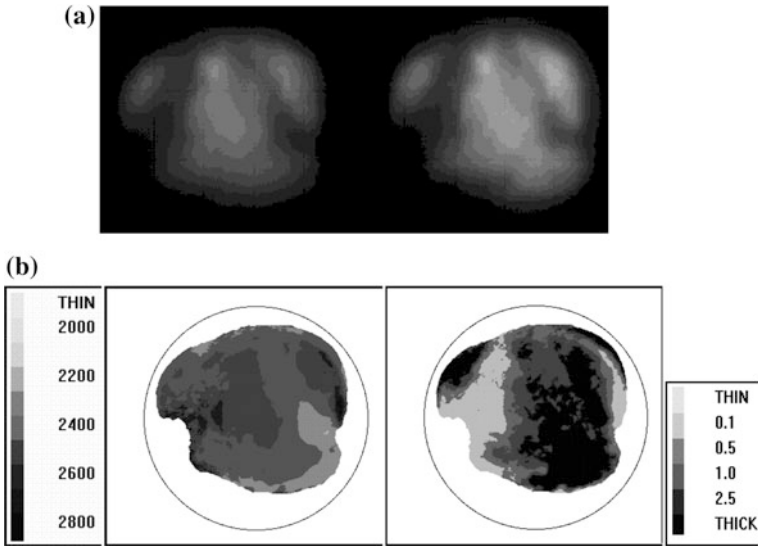


Fig. 25 a Combustion image captured by endoscope, b Temperature and soot distribution obtained from engine endoscopy [31]

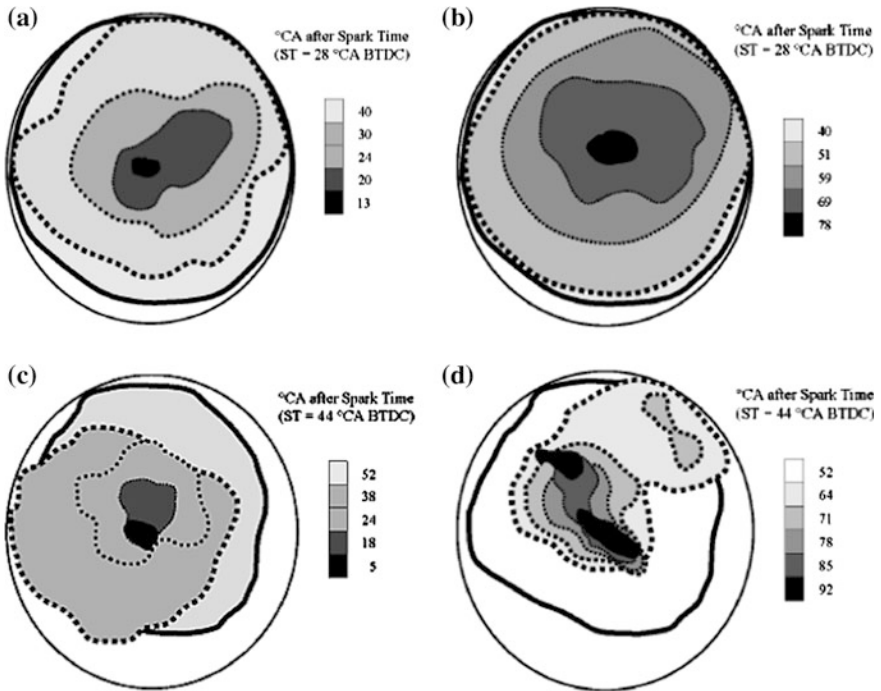


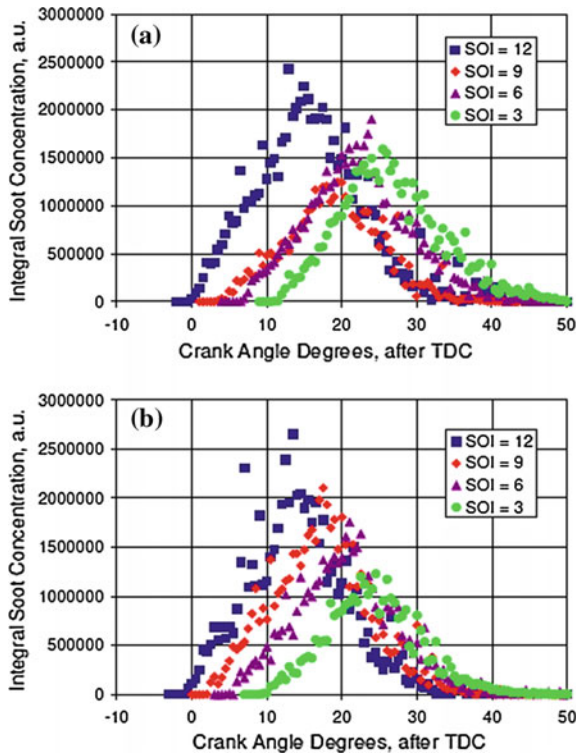
Fig. 26 Flame propagation with stratified charge and homogeneous charge at 1500 rpm and IMEP = 0.2 MPa, a and b Homogeneous; c and d Stratification mode [86]

They found that the peak of soot concentration factor becomes higher at advanced SoI timings (Fig. 27). However in late combustion cycle, soot concentration factor is higher at retarded SoI timings due to decreased turbulence and cylinder pressure, which reduces the soot oxidation rate in late combustion cycles.

In Toyota Motors, Sakata et al. [75] developed a Toyota Reflex Burn (TRB) system to optimize the fuel-air mixing in diesel engines. At that time, gaseous and particulate emissions from small diesel engines created a huge environmental furor. They modified the combustion chamber shape, which generated complex air motion with high turbulence. Endoscope with a camera was used to visualize the mixture formation process, spray and flame behavior to achieve optimum impingement intensity. TBR system generated complex air motion from impingement with the reflex edge in the combustion chamber cavity, which created highly turbulent motion of air. They found that deflection of fuel spray away from the reflex edges reduced wall-wetting, which decreased particulate emissions (Fig. 28).

Nikolic et al. [60] used endoscope in a single cylinder rapid compression machine (RCM), which was used for simulating diesel combustion. They studied the effect of CO₂ concentration, which is used for diluting the intake air in the EGR to control NO_x formation. Soot distribution and ignition properties were analyzed

Fig. 27 Soot concentration factor for four different SoI timings: (a) Diesel, (b) Sun-diesel [57]



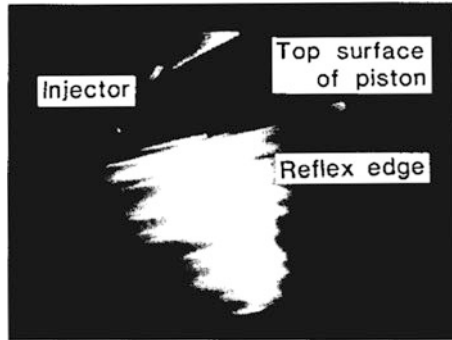


Fig. 28 Combustion cavity captured by endoscopy [75]

with the help of combustion imaging. They captured the combustion images at 0, 4.3, 9.5, 14.3% CO₂ concentrations and compared the combustion and ignition parameters. They found that flame temperature and maximum soot concentration decreased with increasing CO₂ concentration in the intake gas, which made ignition delay longer (Fig. 29).

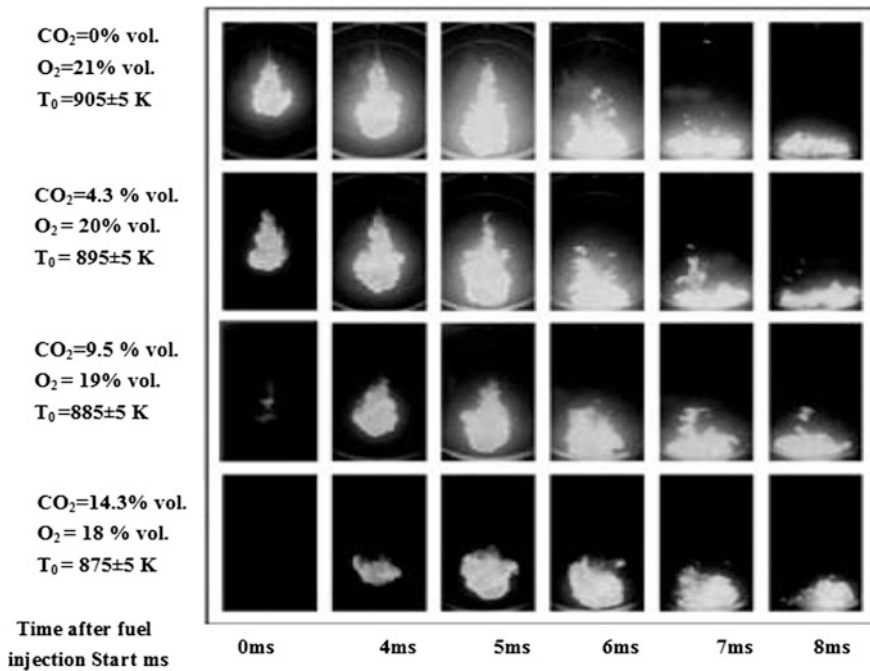


Fig. 29 Diesel spray and combustion images at different conditions [60]

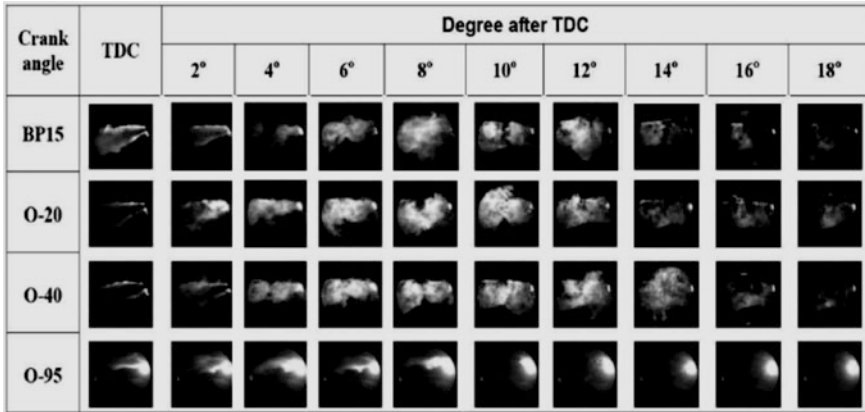
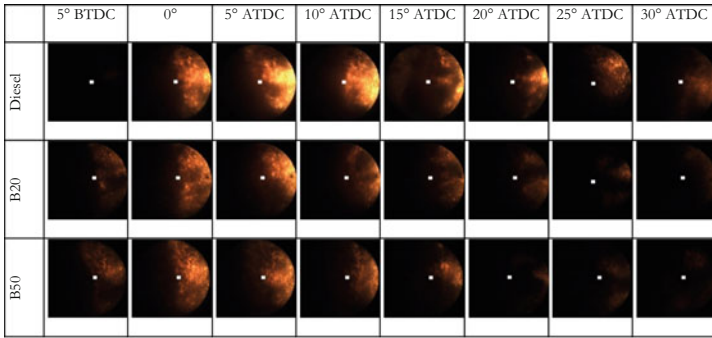


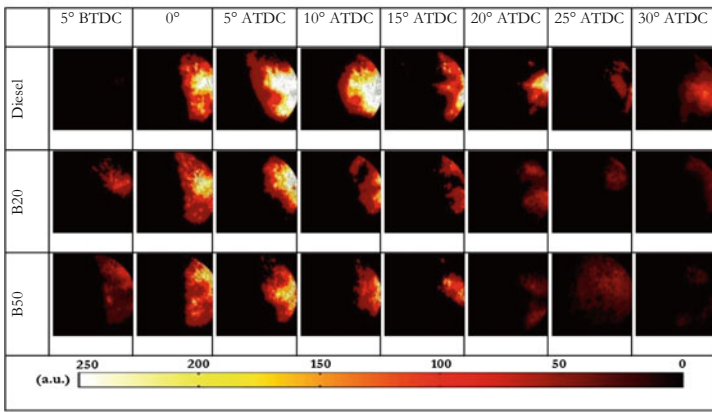
Fig. 30 Spray and combustion images of a DI diesel engine fueled by diglyme-diesel blends [5]

Endoscopic technique is very useful in determining spray characteristics in the engine because this technique provides direct visual access to the combustion chamber and focuses on the nozzle tip. Several studies were carried out for spray visualization, but they were limited to CVSC, but not in a real firing engine, because there were no arrangements for direct access to the belly of the engine which were capable of withstanding high temperature and pressure conditions during combustion. Using endoscopes with lighting arrangement proved to be very helpful for spray analysis in the engine. General cavity endoscopes are used for low light applications. Light is passed through an optical fiber, which is coupled with the endoscope. Alam et al. [5] captured the images of sprays in diesel engine for different blends of dyglyme blended with diesel, namely 20% w/w dyglyme blended with BP15 (“O-20”), 40% w/w dyglyme blended with BP15 (“O-40”) and 95% w/w dyglyme blended with BP15 (“O-95”). They compared the start of injection timings and spray penetration length for these fuels and found that O-20 showed earliest SoI and O-95 showed shortest spray penetration length (Fig. 30).

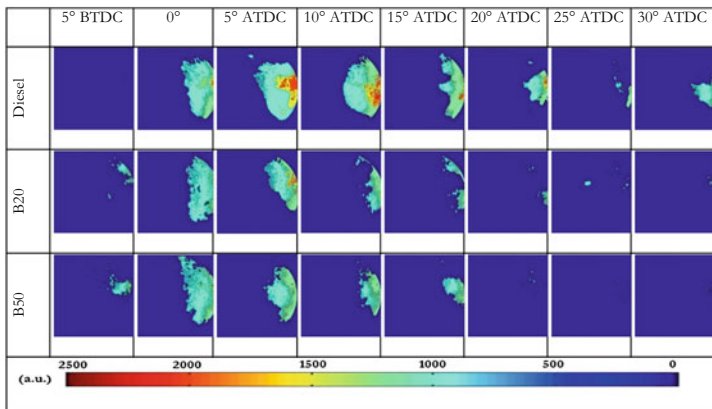
This technique was used for investigating the effect of different parameters on combustion and ignition sites at different engine speeds [71, 73]. Werlberger and Cartellieri [96] used endoscopic high-speed combustion photography in a HSDI engine to investigate the effect of pilot injection on fuel-air mixing and combustion. They also observed the effect of wall temperature on combustion characteristics. Wallner et al. (2007) applied endoscopic technique in a hydrogen fueled DI engine to investigate the effects of fuel injection parameters on fuel-air mixing and combustion characteristics. They found the endoscopic technique to be an excellent tool for in-cylinder combustion diagnostics. Agarwal et al. [2] carried out engine endoscopy in a production grade CI engine fueled by mineral diesel and biodiesel blends and investigated the radiation flame temperature and soot distribution (Fig. 31). They reported that combustion visualization using endoscopy is not effective for highly oxygenated fuels because the intensity and color of the



(a) Spatial and time resolved combustion endoscopy images for different fuels at various positions in an engine cycle



(b) Contours of R intensity for different fuels at various positions in an engine cycle



(c) Spatial and time resolved in-cylinder flame temperature distribution for different fuels at various positions in an engine cycle

Fig. 31 Results of engine endoscopy using mineral diesel and biodiesel blends [2]

combustion images was slightly lower due to lower emission of radiations from unburnt soot particles. They found that higher biodiesel blends led to lower flame temperatures due to lower soot radiations, which indicated higher bulk temperatures. This also justified the higher NO_x formation during biodiesel combustion.

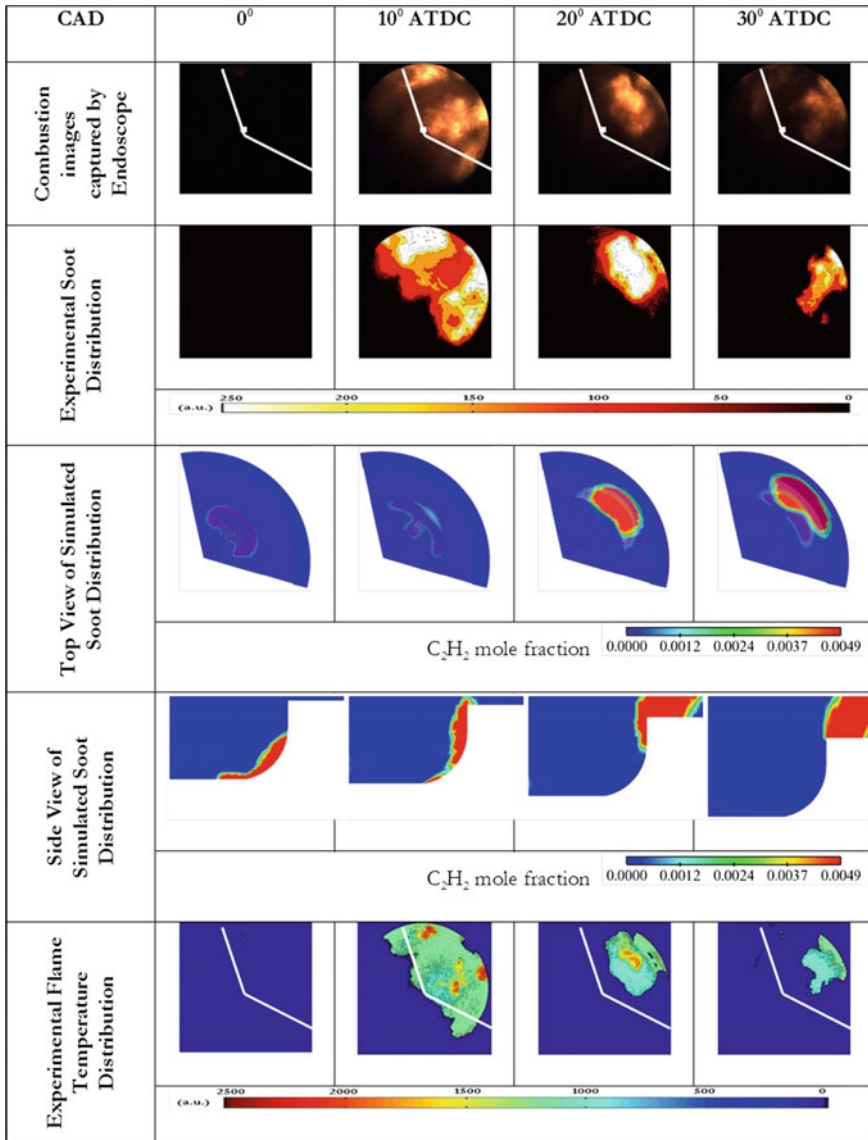


Fig. 32 Comparison of experimental and simulation results of diesel combustion image sequence, spatial soot contours and spatial flame temperature contours at no load [3]

In several studies related to flow pattern analysis, endoscopic technique replaced conventional optical windows due to ease of operation and accessibility. Nauwerck et al. [59] used endoscopic optics to investigate the in-cylinder flow structures during the gas exchange process inside a small two-stroke engine. They successfully implemented this system for PIV under a variety of operating conditions and speeds up to 6000 rpm. Agarwal et al. [3] also compared the engine endoscopy results with simulation results and reported a good agreement between them (Fig. 32).

Schänzlin et al. [77] developed and implemented endoscopic technique for a spray-guided DISI gasoline engine. They examined the in-cylinder behavior to provide optical information on the liquid phase distribution in the combustion chamber at different times after the SoI. They performed numerical analysis for liquid phase distribution and found a good qualitative similarity among them. This technique was also used in multi-cylinder engines fuelled with alternative fuels like alcohols and biofuels to investigate the air-fuel mixing, flow pattern inside the combustion chamber and complex combustion characteristics. Several researchers used this technique for comparing the combustion characteristics of different fuels such as sun-diesel, diesel, diesohol and mineral diesel [57, 95]. Mtui and Hill [58] used endoscopy for investigating ignition delay and combustion duration in a CNG fueled diesel engine. Recently endoscopy was used for various advanced engine applications such as piston temperature evaluation, spray diagnostics, charge flow pattern, flame propagation and mixture formation in SI engines [42].

6 Conclusions

The primary objective of this chapter is to provide an overview of fundamentals and applications of important optical diagnostic techniques for IC engine applications. These techniques are capable of measurements of in-cylinder air-flow characteristics; macroscopic and microscopic spray analysis and combustion diagnostics. A common feature of most optical diagnostics described here is their capability of being non-intrusive and in situ measurements with high spatial and temporal resolution. Hence, these techniques are particularly suited for turbulent flow conditions encountered in IC engines. For each technique, basic theory and the principle were included. For in-cylinder flow analysis, mainly PIV has been used by a large number of researchers. Several new capabilities of advanced configurations of PIV technique such as velocity component analysis, spatial variations of velocity inside the cylinder make this technique even more versatile. Further improvements in combustion process can be achieved by enhancing the fuel-air mixing process by providing a suitable combustion environment and by optimization of parameters that critically influence the combustion. Engine endoscopy is an important optical technique for analysis of engine combustion and spray formation process. It can be used in a wide variety of engine investigations ranging from fuel-air mixing in SI engines to combustion visualization in CI engines. Endoscopy can be also used to

optimize the engine design e.g. shape of the combustion chamber, piston bowl, etc. in addition to analyzing the effect of designs of different components on engine performance, combustion and emission characteristics. Engine endoscopy is widely used for determining spatial flame temperature distribution and spatial soot distribution. Spray visualization in the engine combustion chamber is another important application of endoscopy. Endoscopy offers several advantages in engine experiments due to limited space used for optical access. The applicability of this technique in any production grade engine is another major advantage of endoscopy.

In summary, optical diagnostic techniques have contributed significantly to the knowledge of in-cylinder flow characteristics, fuel-air mixture formation and combustion in IC engines. With ever more stringent emission legislations, use of advanced optical techniques will continue to grow and provide greater understanding of complex air-flows, mixing and combustion phenomena in IC engines.

References

1. Abiola K, Zhu J, Nishida K, Wang X, Huang Z (2013) Characterization of spray and combustion processes of biodiesel fuel injected by diesel engine common rail system. *Fuel* 104:838–846
2. Agarwal AK, Agarwal A, Singh AP (2015) Time resolved in-situ biodiesel combustion visualization using engine endoscopy. *Measurement* 69:236–249
3. Agarwal AK, Singh AP, Agarwal A, Jeon J, Lee CS, Park S (2016) Spatial combustion analysis of biodiesel fueled engine using combustion chamber endoscopy and modeling. *Renew Energy* 98:292–303
4. Agarwal AK, Singh SK, Sinha S, Shukla MK (2004) Effect of EGR on the exhaust gas temperature and exhaust opacity in compression ignition engines. *Sadhana* 29(3):275–284
5. Alam M, Song KH, Boehman A (2005) Spray and combustion visualization of a direct injection diesel engine operated with diglyme fuel blends. *Int J Engine Res* 7:503–521
6. Allen J, Law D, Pitcher G, Williams P (2000) A new optical access research engine for advanced fuel spray and combustion analysis using laser based diagnostics. In: Monograph of 33rd international symposium on automotive technology and automation (ISATA), Dublin, Ireland
7. Ashwood AC, VandenHogen SJ, Rodarte MA, Kopplin CR, Rodríguez DJ, Hurlburt ET, Shedd TA (2015) A multiphase, micro-scale PIV measurement technique for liquid film velocity measurements in annular two-phase flow. *Int J Multiph Flow* 68:27–39
8. Ayati AA, Kolaas J, Jensen A, Johnson GW (2015) Combined simultaneous two-phase PIV and interface elevation measurements in stratified gas/liquid pipe flow. *Int J Multiph Flow* 74:45–58
9. Baum E, Peterson B, Böhm B, Dreizler A (2014) On the validation of LES applied to internal combustion engine flows: Part I: Comprehensive experimental database. *Flow Turbul Combust* 92:269–297
10. Baum E, Peterson B, Surmann C, Michaelis D, Böhm B, Dreizler A (2012) Tomographic PIV measurements in an IC engine. In: 16th international symposium on applications of laser techniques to fluid mechanics, Lisbon, Portugal, 09–12 July 2012
11. Baum E, Peterson B, Surmann C, Michaelis D, Bohmc B, Dreizler A (2013) Investigation of the 3D flow field in an IC engine using tomographic PIV. *Proc Combust Inst* 34:2903–2910

12. Binjuwair SA (2013) Characterization of flow structures inside an engine cylinder under steady state condition. Doctoral thesis, Department of Aeronautical and Automotive Engineering, Loughborough University
13. Bowditch FW (1961) A new tool for combustion research: a quartz piston engine. SAE Paper 610002
14. Chan VSS (2000) Velocity measurement inside a motored internal combustion engine using three-component laser Doppler anemometry. *Opt Laser Technol* 32:557–566
15. Chaves H, Kirmse C, Obermeier F (2001) Velocity measurements of dense diesel sprays in pressurized air. In: *Proceedings of Spray*
16. Choi K, Choi BC, Park H, Joo KJ, Lee JH (2003) In-cylinder flow analysis of a single cylinder DI diesel engine using PIV and CFD. SAE Paper 2003-01-1846
17. Course on IC Engine About Spectroscopy in Optical Engineering Laboratory, University of Warwick. <http://www.eng.warwick.ac.uk/oel/courses/engine/ic029.htm>
18. Dannemann J, Klaas M, Schröder W (2010) Three dimensional flow field within a four valve combustion engine measured by particle-image velocimetry. In: ISFV14—14th international symposium on flow visualization, EXCO Daegu, Korea, 21–24 June 2010
19. Das S, Chmiel DM (2003) Computational and experimental study of in-cylinder flow in a direct injection gasoline (DIG) engine. SAE Paper 2003-01-3083
20. Dent JC (1971) Basis for the comparison of various experimental methods for studying spray penetration. SAE Paper 710571
21. Deslandes W, Dupont A, Georges XB, Boree CJ (2003) PIV measurements of internal aerodynamic of diesel combustion chamber. SAE Paper 2003-01-3083
22. Dierksheide U, Meyer P, Hovestadt T, Hentschel W (2002) Endoscopic 2D particle image velocimetry (PIV) flow field measurements in IC engines. *Exp Fluids* 33:794–800
23. Docquier N, Candel S (2008) Combustion control and sensors: a review. *Prog Energy Combust Sci* 28:17–150
24. Ejim C, Fleck B, Amirfazli A (2007) Analytical study for atomization of biodiesels and their blends in a typical injector: surface tension and viscosity effects. *Fuel* 86:1534–1544
25. Elkotb MM (1982) Fuel atomization for spray modeling. *Prog Energy Combust Sci* 61–91
26. Faeth GM, Hsiang LP, Wu PK (1995) Structures and breakup properties of sprays. *Int J Multiph Flow* 21:9–127
27. Gadekar S, Singh AP, Agarwal AK (2016a) Tomographic PIV evaluation of in-cylinder flow evolution and effect of engine speed. SAE Paper 2016-01-0638
28. Galle J, Demuyneck J, Vancouille J, Verhelst S (2012) Spray parameter comparison between diesel and vegetable oils for non-evaporating conditions. SAE Paper 2012-01-0461
29. Gao Y, Deng J, Li C, Dang F, Liao Z, Wu Z et al (2009) Experimental study of the spray characteristics of biodiesel based on inedible oil. *Biotechnol Adv* 27:616–624
30. Ghurri A, Jae-duk K, Kyu-Keun S, Jae-Youn J, Hyung GK (2011) Qualitative and quantitative analysis of spray characteristics of diesel and biodiesel blend on common-rail injection system. *J Mech Sci Technol* 25:885–893
31. Hampson GJ, Reitz RD (1998) Two-color imaging of in-cylinder soot concentration and temperature in a heavy-duty DI diesel engine with comparison to multidimensional modeling for single and split injections. SAE Paper 980524
32. Han YT, Ki-bum K, Lee G (2008) The investigation of soot and temperature distributions in a visualized direct injection diesel engine using laser diagnostics. *Meas Sci Technol* 19:115402–115412
33. Handbook: Henein NA, Patterson DJ (1972) Emissions from combustion engine and their control. Ann Arbor Science Publishers, Ann arbor, MI
34. Handbook: Heywood JB (1988) Internal combustion engine. McGraw-Hill Book Company, New York
35. Handbook: Majewski WA, Khair MK (2006) Diesel emission and their control. SAE International, pp 367–377
36. Handbook: Pundir BP (2010) IC engines: combustion and emissions. Narosa Publishing House, New Delhi

37. Handbook: Raffel M, Willert CE, Wereley S, Kompenhans J (2007) Particle image velocimetry, a practical guide. Springer, Berlin, Heidelberg
38. He C, Ge Y, Tan J, Han X (2008) Spray properties of alternative fuels: a comparative analysis of biodiesel and diesel. *Int J Energy Res* 32:1329–1338
39. Hiroyasu H, Arai M (1990) Structures of fuels sprays in diesel engines. SAE Paper 1990-90-0475
40. Huang RF, Huang CW, Chang SB, Yang HS, Lina TW, Hsub WY (2005) Topological flow evolutions in cylinder of a motored engine during intake and compression strokes. *J Fluids Struct* 20:105–127
41. Huang Z, Lu H, Jiang D, Zeng K, Liu B, Zhang J, Wang X (2004) Combustion behaviors of a compression-ignition engine fuelled with diesel/methanol blends under various fuel delivery advance angles. *Bioresour Technol* 95(3):331–341
42. Husberg T, Gjrja S, Denbratt I (2005) Piston temperature measurement by use of thermographic phosphors and thermocouples in a heavy-duty diesel engine run under partly premixed conditions. SAE Paper 2005-01-1646
43. Julien L (2006) Characteristics of diesel sprays at high temperatures and pressures. PhD thesis, University of Brighton, UK
44. Justham T, Jarvis S, Clarke A, Garner CP, Hargrave GK, Halliwell NA (2006) simultaneous study of intake and in-cylinder IC engine flow fields to provide an insight into intake induced cyclic variations. *J Phys: Conf Ser* 45:146–153
45. Kawaguchi Y, Segawa T, Feng Z, Li P (2002) Experimental study on drag-reducing channel flow with surfactant additives—spatial structure of turbulence investigated by PIV system. *Int J Heat Fluid Flow* 23:700–709
46. Kim YD, Lee SY (2002) Application of Hough transform to image processing of heavily overlapped particles with spherical shapes. *Atomization Sprays* 12:451–461
47. Kim HJ, Park SH, Lee CS (2010) A study on the macroscopic spray behavior and atomization characteristics of biodiesel and dimethyl ether sprays under increased ambient pressure. *Fuel Process Technol* 91:354–363
48. Koch T, Schänzlin K, Boulouchos K (2002) Characterization and phenomenological modeling of mixture formation and combustion in a direct injection spark ignition engine. SAE Paper 2002-01-1138
49. Koh KU, Kim JY, Lee SY (2001) Determination of in-focus criteria and depth field in image processing of spray particles. *Atomization Sprays* 11:317–333
50. Lee CS, Park SW (2002) An experimental and numerical study on fuel atomization characteristics of high-pressure diesel injection sprays. *Fuel* 81:2417–2423
51. Lee CS, Reitz RD (2004) Investigation of spray characteristics from a low-pressure common rail injector for use in a homogeneous charge compression ignition engine. *Meas Sci Technol* 15:509–519
52. Lee J, Farrell PV' (1993) Intake valve flow measurements of an IC engine using particle image velocimetry. SAE 930480
53. Lefebvre AH (1989) *Atomization and sprays*, vol 12. Hemisphere
54. Manual: Operation of the phase doppler interferometer (PDI) for spray drop size and velocity measurement. Artium Technologies
55. Manual: Tomographic PIV, volumetric flow field imaging. Lavision, Germany
56. Metghalchi M, Keck JC (1982) Burning velocities of mixtures of air with methanol, isooctane, and indolene at high pressure and temperature. *Combust Flame* 48(1982):191–210
57. Miers SA, Ng H, Ciatti SA (2005) Emissions, performance, and in-cylinder combustion analysis in a light-duty diesel engine operating on a fischer-tropsch, biomass-to-liquid fuel. SAE Paper 2005-01-3670
58. Mtui PL, Hill PG (1996) Ignition delay and combustion duration with natural gas fueling of diesel engines. SAE Paper 961933
59. Nauwerck, A, Gindele J, Spicher U, Rosskamp H (2000) Investigation of the transient in-cylinder flow inside a two stroke engine with particle-image-velocimetry. SAE Paper 2000-01-0902

60. Nikolic D, Iida N (2007) Effects of intake CO₂ concentrations on fuel spray flame temperatures and soot formations. *J Automobile Eng Proc IMech E* 221:1567
61. Nishiyama A, Jeong H, Ikeda Y, Sawada R (2012) Application of endoscopic stereo PIV to 3D exhaust gas flow: measurements in a practical SI engine. In: 16th International symposium on applications of laser techniques to fluid mechanics, Lisbon, Portugal
62. Park SH, Kim HJ, Suh HK, Lee CS (2009) Experimental and numerical analysis of spray-atomization characteristics of biodiesel fuel in various fuel and ambient temperatures conditions. *Int J Heat Fluid Flow* 30:960–970
63. Park SH, Yoon SH, Lee CS (2011) Effects of multiple-injection strategies on overall spray behavior, combustion, and emissions reduction characteristics of biodiesel fuel. *Appl Energy* 88:88–98
64. Park SH, Youn IM, Lim Y, Lee CS (2013) Influence of the mixture of gasoline and diesel fuels on droplet atomization, combustion, and exhaust emission characteristics in a compression ignition engine. *Fuel Process Technol* 106:392–401
65. Park SW, Lee CS (2003) Macroscopic structure and atomization characteristics of high-speed diesel spray. *Int J Automot Technol* 4:157–164
66. Pastor JV, Garcia M, Molina S (2000) Analysis methodology of diesel spray and flame by means of in-cylinder endoscopic imaging. *IEEE Savoy Place, London*, vol 80
67. Perini F, Miles PC, Reitz RD (2014) A comprehensive modeling study of in-cylinder fluid flows in a high-swirl, light-duty optical diesel engine. *Comput Fluids* 105:113–124
68. Postrioti L; Grimald C, (2000) Experimental comparison between conventional and bio-derived fuels sprays from a common rail injection system, SAE 2000-01-1252
69. Reeves M, Garner CP, Dent JC, Halliwell NA (1996) Particle image velocimetry analysis of ic engine in-cylinder flows. *Opt Lasers Eng* 25:415–432
70. Rhodes DB, Keck JC, Burnign L (1985) Speed measurements of indolene-air-diluent mixtures at high pressures and temperature. SAE Paper 850047
71. Ricart LM, Xin J, Bower GR, Reitz RD (1997) In-cylinder measurement and modelling of liquid fuel spray penetration in a heavy-duty diesel engine. SAE Paper 971591
72. Richter M, Axelsson B, Aldén M, Josefsson G, Carlsson LO, Dahlberg M, Nisbet J, Simonsen H (1999) Investigation of the fuel distribution and the in-cylinder flow field in a stratified charge engine using laser techniques and comparison with CFD modeling. SAE Paper 1999-01-3540
73. Ryan TW, Shahed SM (1994) Injection pressure and intake air density effects on ignition and combustion in a 4-valve diesel engine. SAE Paper 941919
74. Sakaguchi D, Amida OL, Ueki H, Ishida M (2008) Measurement of droplet size distribution in core region of high-speed spray by micro-probe L2F. *J Therm Sci* 17:90–96
75. Sakata I, Ishisaka K, Yanagihara H, Sami H (1990) Development of TOYOTA reflex burn (TRB) system in DI diesel. SAE Paper 900658
76. Sasaki S, Akagawa H, Tsujimura K (1998) A study on surrounding air flow induced by diesel sprays. SAE Paper 980805
77. Schänzlin K, Koch T, Tzannis A, Boulouchos K (2001) Characterization of mixture formation in a direct injected spark ignition engine. SAE Paper 2001-01-1909
78. Schodl R (1974) L₂F a laser-dual-beam method for flow measurements in turbomachines. ASME Paper No.74, GT-157
79. Schunemann E, Fedrow S, Leipertz A (1998) Droplet size and velocity measurements for the characterization of a DI-diesel spray impinging on a flat wall. SAE Paper 982345
80. Singh AP, Gadekar S, Agarwal AK (2016b) In-cylinder air-flow characteristics using tomographic PIV at different engine speeds, intake air temperatures and intake valve deactivation in a single cylinder optical research engine. SAE Paper 2016-28-0001
81. Singh AP, Gupta A, Agarwal AK (2015) Tomographic particle image velocimetry for flow analysis in a single cylinder optical engine. *SAE Int J Mater Manuf* 8(2):472–481
82. Som S, Longman DE, Ramírez AI, Aggarwal SK (2010) A comparison of injector flow and spray characteristics of biodiesel with petrodiesel. *Fuel* 89:4014–4024

83. Son SY, Kihm KD, Han JC (2002) PIV flow measurements for heat transfer characterization in two-pass square channels with smooth and 90 ribbed walls. *Int J Heat Mass Transf* 45:4809–4822
84. Spicher U, Kölmel A, Kubach H, Töpfer G (2000) Combustion in spark ignition engines with direct injection. SAE Paper 2000-01-0649
85. Stucky MJ, Nino E, Gajdeczko B, Felton PG (1994) Two-color particle image velocimetry technique for an internal combustion engine. *Exp Thermal Fluid Sci* 8:305–314
86. Subramaniam S, Ganesan V, Rao SP, Sampath S (1990) Turbulent flow inside the cylinder of a diesel engine—an experimental investigation using hot wire anemometer. *Exp Fluids* 9:167–174
87. Suh HK, Roh HG, Lee CS (2008) Spray and combustion characteristics of biodiesel/diesel blended fuel in a direct injection common-rail diesel engine. *J Eng Gas Turbines Power* 130:032807
88. Sun JH, Yates A, Winterbone DE (1996) Measurement of flow field in diesel engine combustion chamber after combustion by cross correlation method. *Exp Fluids* 20:335–345
89. Sweetland P, Reitz RD (1994) Particle image velocimetry measurements in the piston bowl of a DI diesel engine. SAE Paper 940283
90. Tanaka T, Narahara K, Tabata M, Yoshiyama S, Tomita E (2005) Ion current measurement in a homogeneous charge compression ignition engine. *Int J Engine Res* 6:453–463
91. Valentino G, Kaufman D, Farrell P (1993) Intake valve flow measurements using PIV. SAE Paper 932700
92. Wang X, Huang Z, Kuti OA, Zhang W, Nishida K (2010) Experimental and analytical study on biodiesel and diesel spray characteristics under ultra-high injection pressure. *Int J Heat Fluid Flow* 31:659–666
93. Wattanavichien K, Azetsu, A (2004) Studies of visualized diesohol combustion phenomena in IDI engine. In: *The international symposium on diagnostics and modeling of combustion in internal combustion engines 2004*, vol 6, pp 423–430, 2004-08-02
94. Werlberger P, Cartellieri W (1987) Fuel injection and combustion phenomena in a high speed DI diesel engine observed by means of endoscopic high speed photography. SAE Paper 870097
95. Wernert P, Koerber G, Wietrich F, Raffel M, Kompenhans J (1997) Demonstration by PIV of the non-reproducibility of the flow field around an airfoil pitching under deep dynamic stall conditions and consequences. *Aerosp Sci Technol* 2:125–135
96. Xu D, Chen J (2013) Accurate estimate of turbulent dissipation rate using PIV data. *Exp Thermal Fluid Sci* 44:662–672
97. Zentgraf F, Baum E, Böhm B, Dreizler A, Peterson B (2014) Analysis of the turbulent in-cylinder flow in an IC engine using tomographic and planar PIV measurements. In: *17th international symposium on applications of laser techniques to fluid mechanics*, Lisbon, Portugal, 07–10 July 2014
98. Zhang X, Su G, Yu J, Yao Z, He F (2015) PIV measurement and simulation of turbulent thermal free convection over a small heat source in a large enclosed cavity. *Build Environ* 90:105–113